Supporting Information:

Analyzing fidelity and reproducibility of DNA templated plasmonic nanostructures

Divita Mathur,[†,a,d] William P. Klein,[†,a,c] Matthew Chiriboga,[a,e] Hieu Bui,[a,c] Eunkeu Oh,[b,f] Rafaela Nita,[a,c] Jawad Naciri,[a] Paul Johns,[a,g] Jake Fontana,[a] Sebastián A. Díaz,[a] and Igor L. Medintz[a*]

[a.] *Center for Bio/Molecular Science and Engineering Code 6900, and*
[b.] *Optical Sciences Division Code 5600, U.S. Naval Research Laboratory, 4555 Overlook AV SW, Washington, DC 20375, USA.*
[c.] *National Research Council, 500 5th St NW, Washington, DC 20001, USA.*
[d.] *College of Science and*
[e.] *Department of Bioengineering, Institute for Advanced Biomedical Research, George Mason University, Fairfax, VA 22030, USA.*
[f.] *KeyW Corporation, Hanover, MD 21076, USA.*
[g.] *American Society for Engineering Education, 1818 N Street NW, Suite 600, Washington, DC 20036, USA.*
† Authors contributed equally.
* igor.medintz@nrl.navy.mil

Supporting Information S1: DNA origami nanostructures

DNA triangle design

The DNA origami triangle is based on the original design by Paul Rothemund.[1] **Figure S1** shows a two-dimensional caDNAno[2] rendering of the DNA triangle wherein each side is designated as A, B, or C, and the staple strands within each side are assigned a number. Staple strands are addressed by the side+number; for example, A08 is staple 8 in side A. All the staple strands required to form the DNA triangle are listed in **Table S1**.

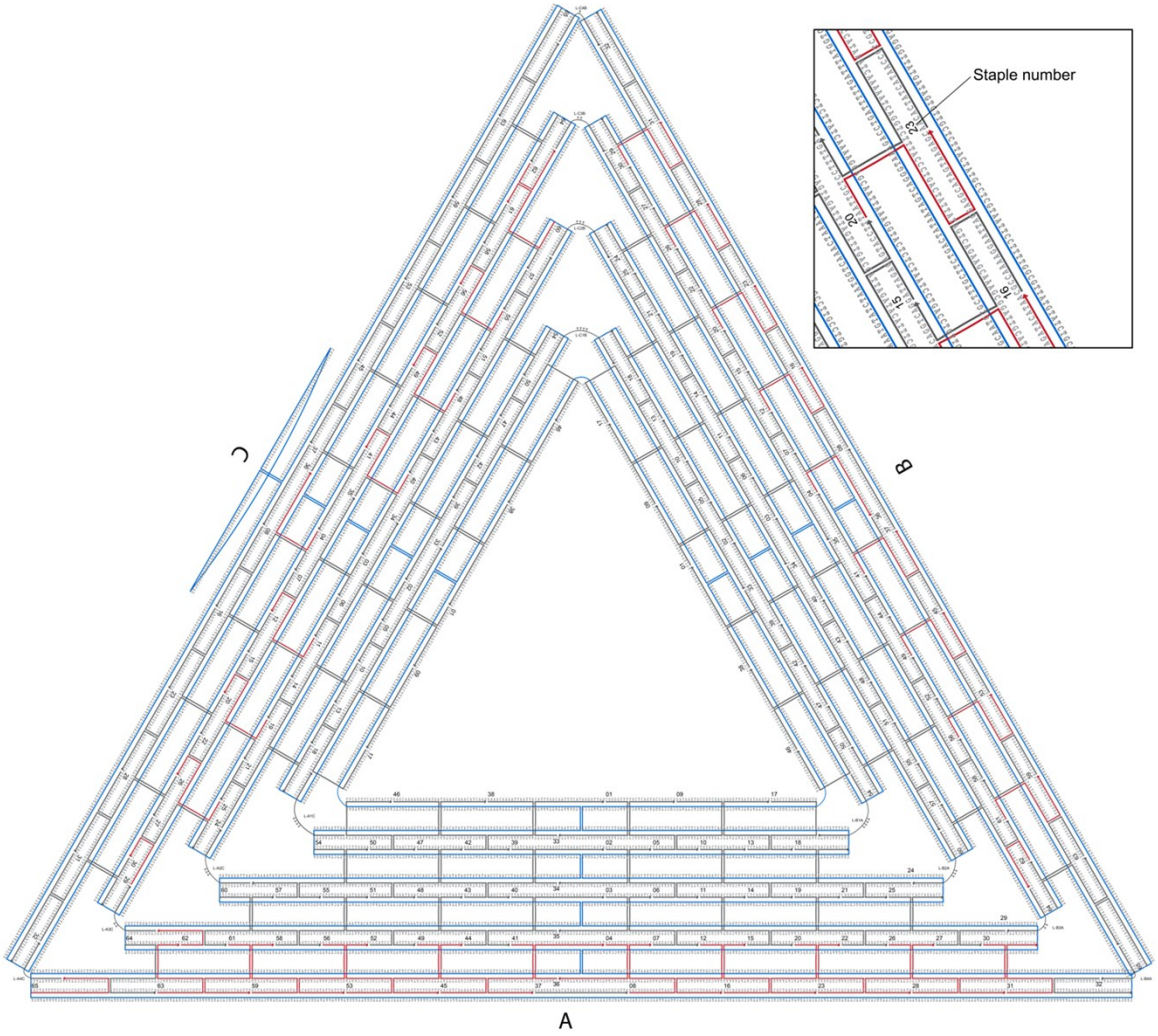

Figure S1: A high-resolution caDNAno rendering of the DNA Triangle. The scaffold strand is shown in blue while the staple strands are in grey or red. Red staple strands represent modified strands that were substituted with either AuNR/AuNP capture strands or bridge strands to form the DNA rhombus. Each side is designated A, B, or C, and the staple strands are numbered along each side; sequences of which can be found in **Table S1**.

DNA rhombus design

The DNA rhombus is formed by bridging two DNA triangles using bridge staple strands (**Table S2**). The bridge staple strands bring together side B on each triangle, thus sides A and C form the outer edges of the rhombus with diagonal symmetry (sides A of each triangle are diagonally opposite to each other), as shown in **Figure S2**.

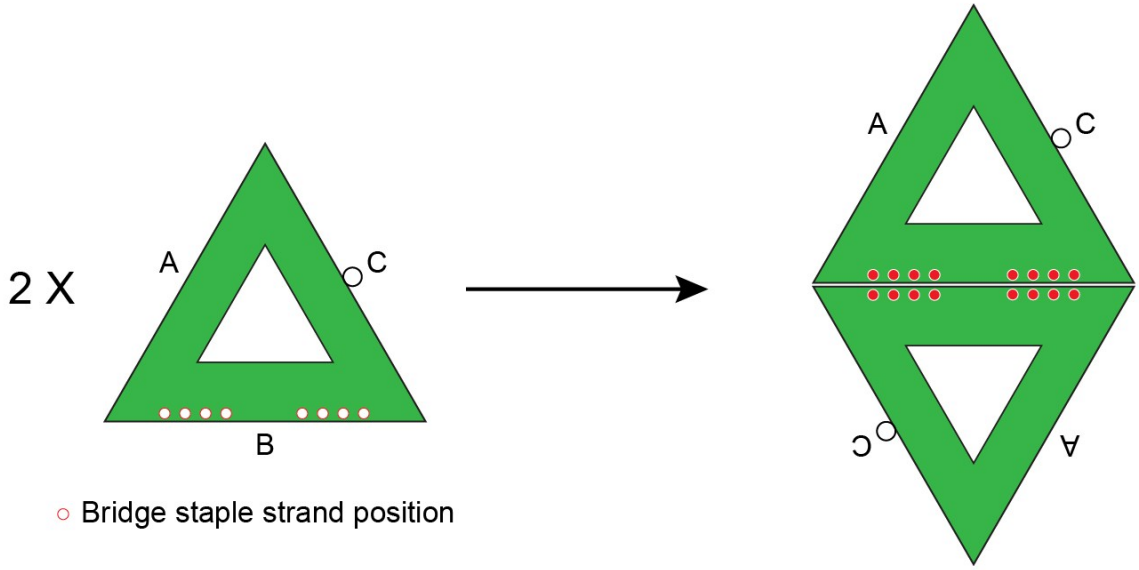

Figure S2: Schematic representing the formation process of the DNA rhombus from the DNA triangle. Eight staple strands along side B were replaced with bridge staple strands that allow the joining of two identical triangles.

Supporting Information S2: DNA nanostructure FPLC purification

DNA triangle purification by FPLC

Scaling up of the production of AuNR-DNA nanostructure complexes required the synthesis of large quantities of DNA origami triangle, made possible by FPLC-based purification. DNA origami triangle and rhombus were assembled on the order of 40 to 120 pmoles. The volume of assembled nanostructure was reduced to 200 to 500 uL using Amicon ultracentrifugation spin columns (100 kDa MWCO), followed by FPLC elution. FPLC running buffer was 50 mM HEPES 4.5 mM $MgCl_2$ 250 mM NaCl and the flow rate was set to 0.5 mL/min. **Figure S3** shows an FPLC absorbance spectrum and fraction collection profile of the DNA triangle. The first peak to be eluted represents the formed DNA origami triangle whereas the second wider peak represents excess staple strands. Fractions corresponding to the nanostructure were collected, combined, and buffer exchanged back to the working buffer conditions (50 mM HEPES 9 mM $MgCl_2$) using Amicon ultracentrifugation filter columns (100 kDa MWCO).

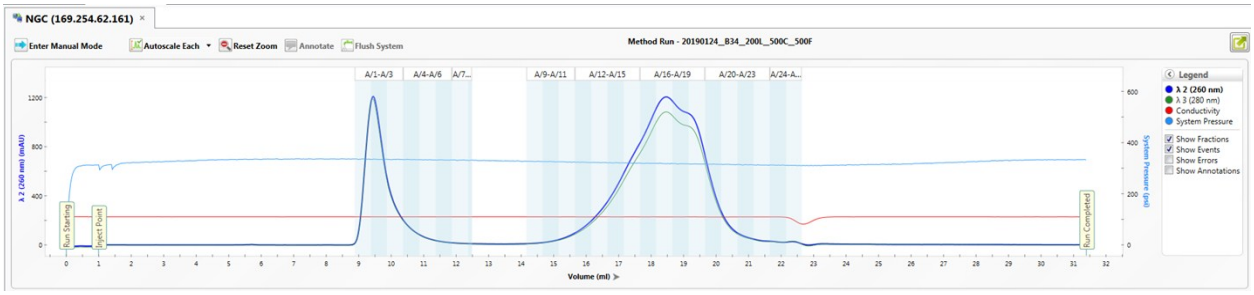

Figure S3: Absorbance spectra generated during FPLC fraction collection of the DNA triangle. The x-axis represents elution volume over time and the y-axis represents absorbance (mA) at 260 nm. The FPLC was programed to collect fractions (A/1, A/2,…) of elution absorbance of > 10 mA, shown as dark and light blue vertical bands. After the completion of the program, fractions A1-A3 were collected and combined to recover the formed DNA triangle whereas the remaining fractions, representing excess staple strands, were discarded.

DNA rhombus purification by FPLC

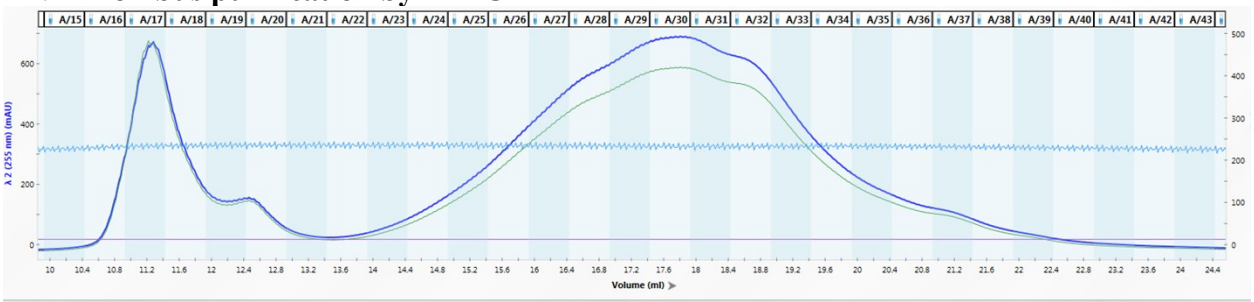

Figure S4: Absorbance spectra generated during FPLC fraction collection of the DNA rhombus. The x-axis represents elution volume over time and the y-axis represents absorbance (mA) at 255 nm. The FPLC was programed to collect fractions (A/1, A/2,…) shown as dark and light blue vertical bands. After the completion of the program, fractions corresponding to the first peak (A16-A18 in this example) were collected and combined to recover the formed DNA rhombus whereas the remaining fractions, representing single triangles and excess staple strands, were discarded.

Supporting Information S3: AuNP and AuNR synthesis

AuNP synthesis

Gold nanoparticles stabilized with sodium citrate with a diameter of 10 nm were synthesized following published procedures with some modifications.[3] Briefly, 200 µL (2.0×10^{-5} mol) of 0.1 M tetrachloroauric (III) acid ($HAuCl_4 \cdot 3H_2O$) aqueous stock solution was mixed with 50 µL (1.0×10^{-5} mol) of 0.2 M of sodium citrate dihydrate stock solution in 50 mL of deionized H_2O under vigorous stirring. After 1 min of stirring the mixture, 400 µL (4.0×10^{-5} mol) of 0.1 M cold sodium borohydride ($NaBH_4$) stock solution in deionized water was added quickly to the reaction mixture and kept at room temperature for the next 3 hours to complete the reaction. NP concentration was determined.[4-6] The final NP sizes were confirmed by TEM measurement.

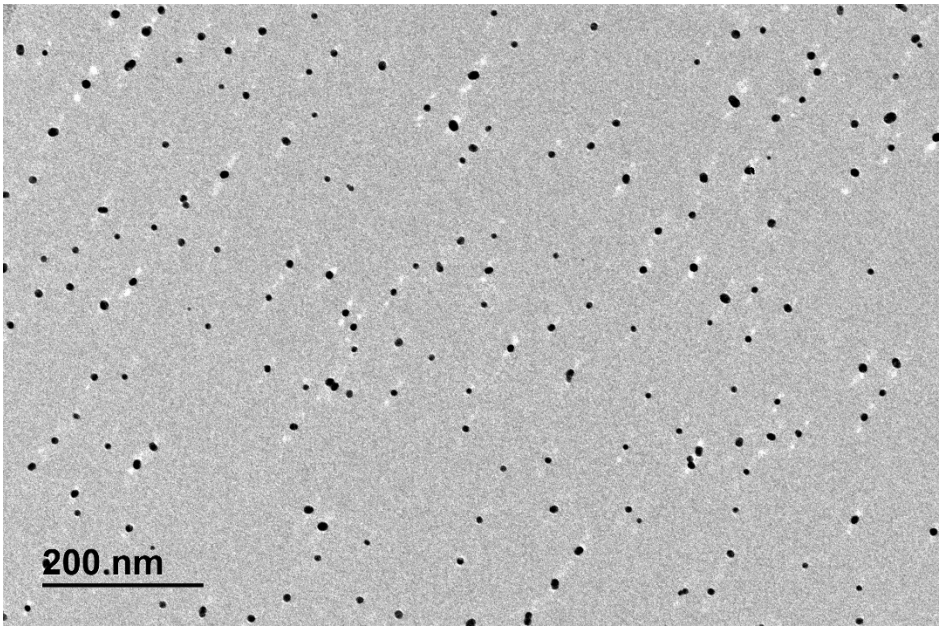

Figure S5: Representative TEM image of 10 nm AuNPs.

AuNR synthesis

The 10x90 nm AuNRs were synthesized by a modified seed mediated growth process in CTAB/BDAC solutions in the presence of $HAuCl_4$, as reported previously.[7] The 20 X 50 nm AuNRs were prepared following the seed mediated method as described earlier.[8]

Purification of the DNA functionalized AuNP and AuNR

After functionalization, the thiol-DNA-AuNR solution was subjected to centrifugation at 9,000 rcf for 30 min at 20°C. The supernatant containing unbound thiol-DNA was discarded and the pellet was collected and transferred to a 2 mL vial. 80% glycerol solution (gel loading solution) was added to the AuNR pellet to bring to a final concentration of ~40%. This solution was loaded into a 0.8% agarose gel in 1X TBE (pH 8.4) and subjected to electric current at 100-120 V/cm for 2-3 h. **Figure S6** shows the result of gel electrophoresis on 20 X 50 nm AuNR functionalized with

A-seq thiolated-DNA. The band representing functionalized AuNR was then excised and extracted using parafilm-coated glass slides.

Gel purification of AuNRs

A

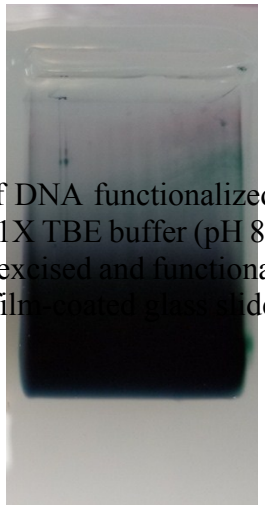

B

Figure S6: Purification of DNA functionalized (A) 20 X 50 nm and (B) 10 X 90 nm AuNR by AGE. 0.8% agarose gel in 1X TBE buffer (pH 8.4) was run at 100-120 V/cm for 2-[illegible] tangular regions marked here were excised and functionalized AuNRs were recovered by applying pressure on gel band between parafilm-coated glass slides.

Magnesium Screening test on functionalized 20 X 50 nm AuNRs

We included the magnesium screening in the standard protocol in order to determine functionalized AuNR stability in the presence of Mg^{2+}, an important component in DNA origami stability.[9] The screening was conducted by adding 1 µL of the functionalized AuNRs to a series of $MgCl_2$ droplets (~30 µL) with an increasing amount of $MgCl_2$, typically in the range of 0 mM to 500 mM. Characterization of stability was based on a visual change in the color of the droplets (**Figure S6**). Grey to clear droplets indicated that the AuNRs had crashed or aggregated and were not stable at that particular $MgCl_2$ concentration. Only DNA-functionalized AuNRs stable at a minimum of 50 mM $MgCl_2$ were further used in the experiments. Even though the $MgCl_2$ concentration typically used for DNA nanostructure stability does not exceed 20 mM, in our experience, the threshold of 50 mM in the magnesium screening ensured consistent and high attachment yields.

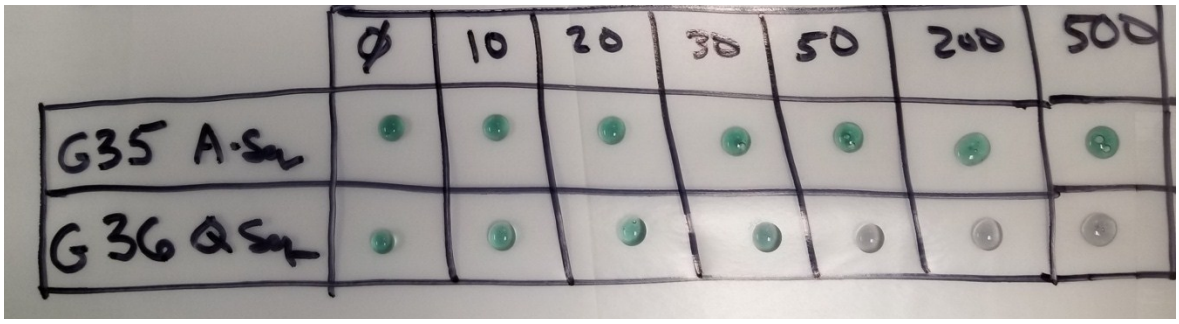

Figure S7: Magnesium screening of 20 X 50 nm AuNRs functionalized with A-seq or Q-seq. Each droplet of liquid shown here represents 1 µL of AuNR mixed in 30 µL of $MgCl_2$ at various concentrations. The columns represent $MgCl_2$ concentration (mM). Change of color to grey in case of batch "G36" Q-seq indicates loss of stability.

Supporting Information S4: Purification of NP-DNA origami constructs

AGE purification of ETE DNA triangle-AuNR constructs

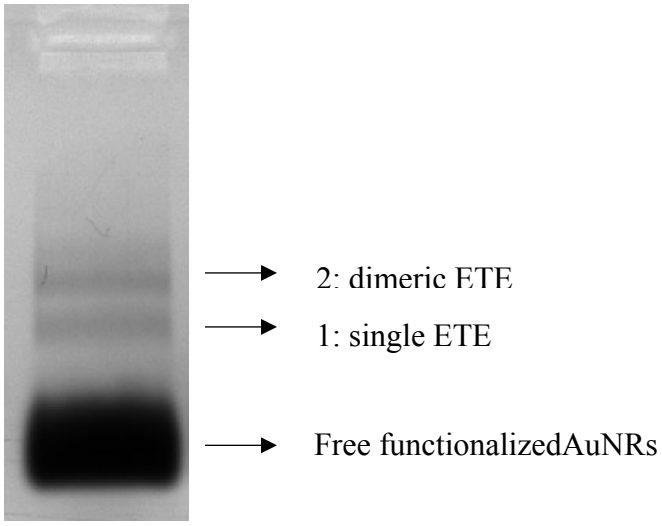

Figure S8: Purification of AuNR-DNA triangle ETE structures by AGE. Gel separation resulted in three primary products shown here as three distinct gel bands. The fastest band represents excess unbound functionalized AuNRs whereas the slowest and middle bands represent ETE dimeric and single triangle constructs, respectively. Gel conditions: 0.8% agarose gel in 50 mM HEPES 9 mM $MgCl_2$, run at 70-80 V/cm at 4°C in an ice bath.

AGE purification of RPR DNA triangle-AuNR constructs

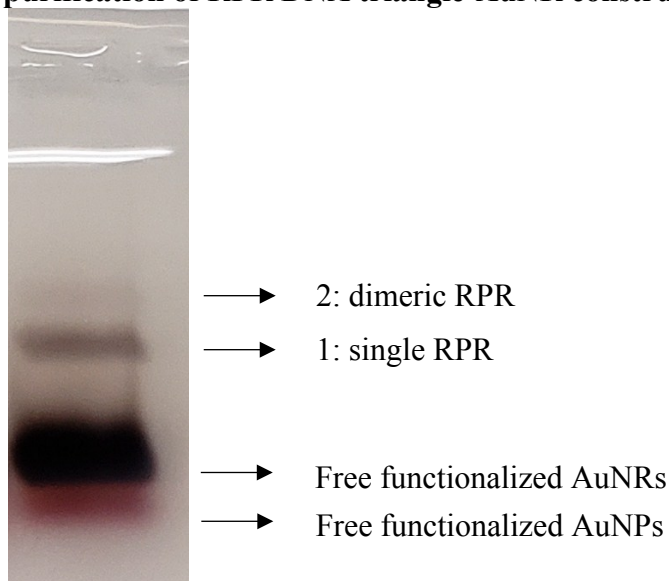

Figure S9: Purification of AuNR-DNA triangle RSR structures by AGE. Gel separation resulted in four primary products shown here as three distinct gel bands. The fastest band represents excess unbound functionalized AuNPs whereas the slowest and second bands represent RPR dimeric and single triangle constructs, respectively. Gel conditions: 0.8% agarose gel in 50 mM HEPES 9 mM $MgCl_2$, run at 70-80 V/cm at 4°C in an ice bath.

Supporting Information S5: AFM images of each configuration

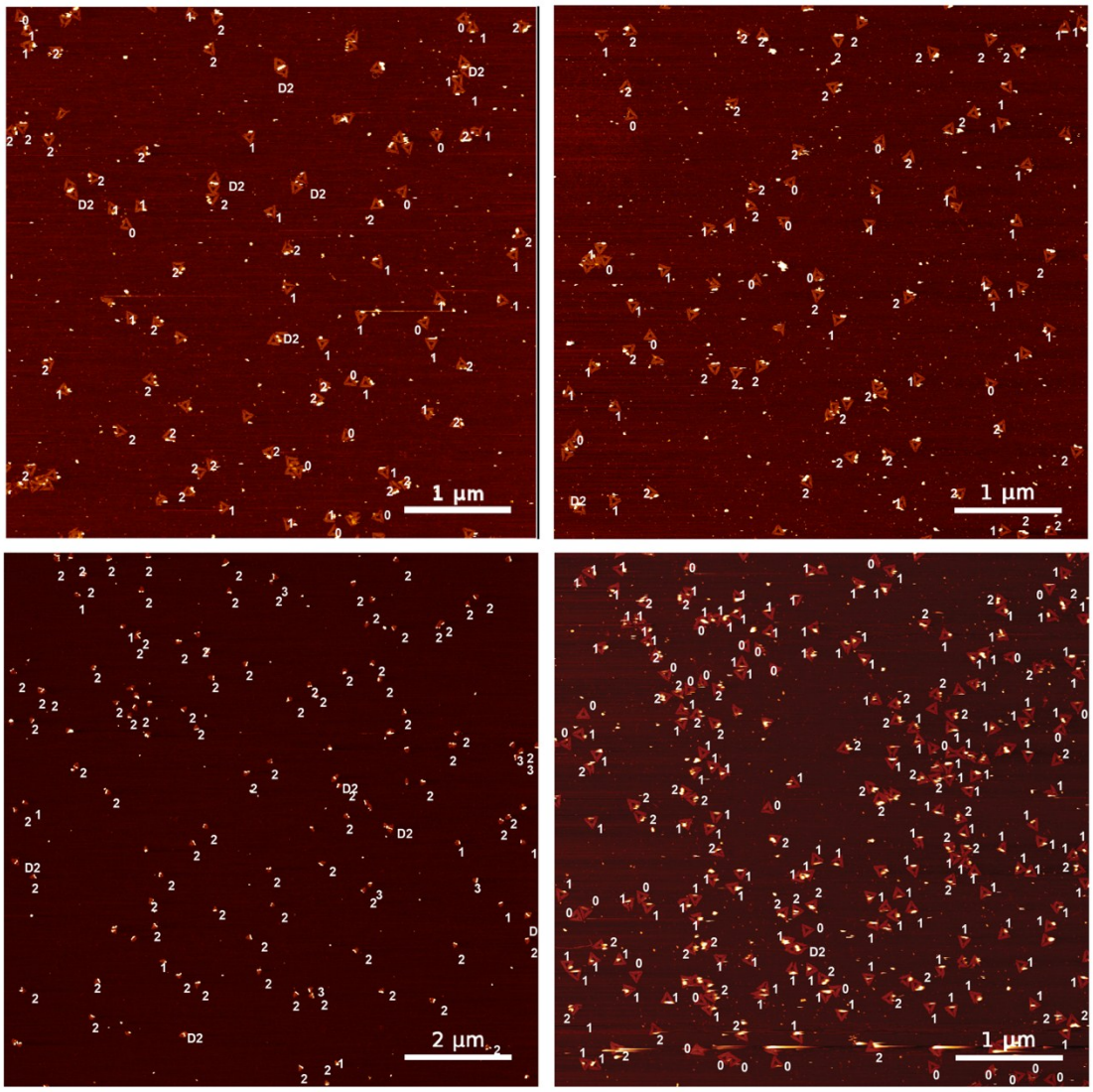

Figure S10: Representative AFM images of 20 X 50 nm AuNR ETE single DNA triangle construct, including particle count analysis, the summary of which is shown in main text Figure 3.

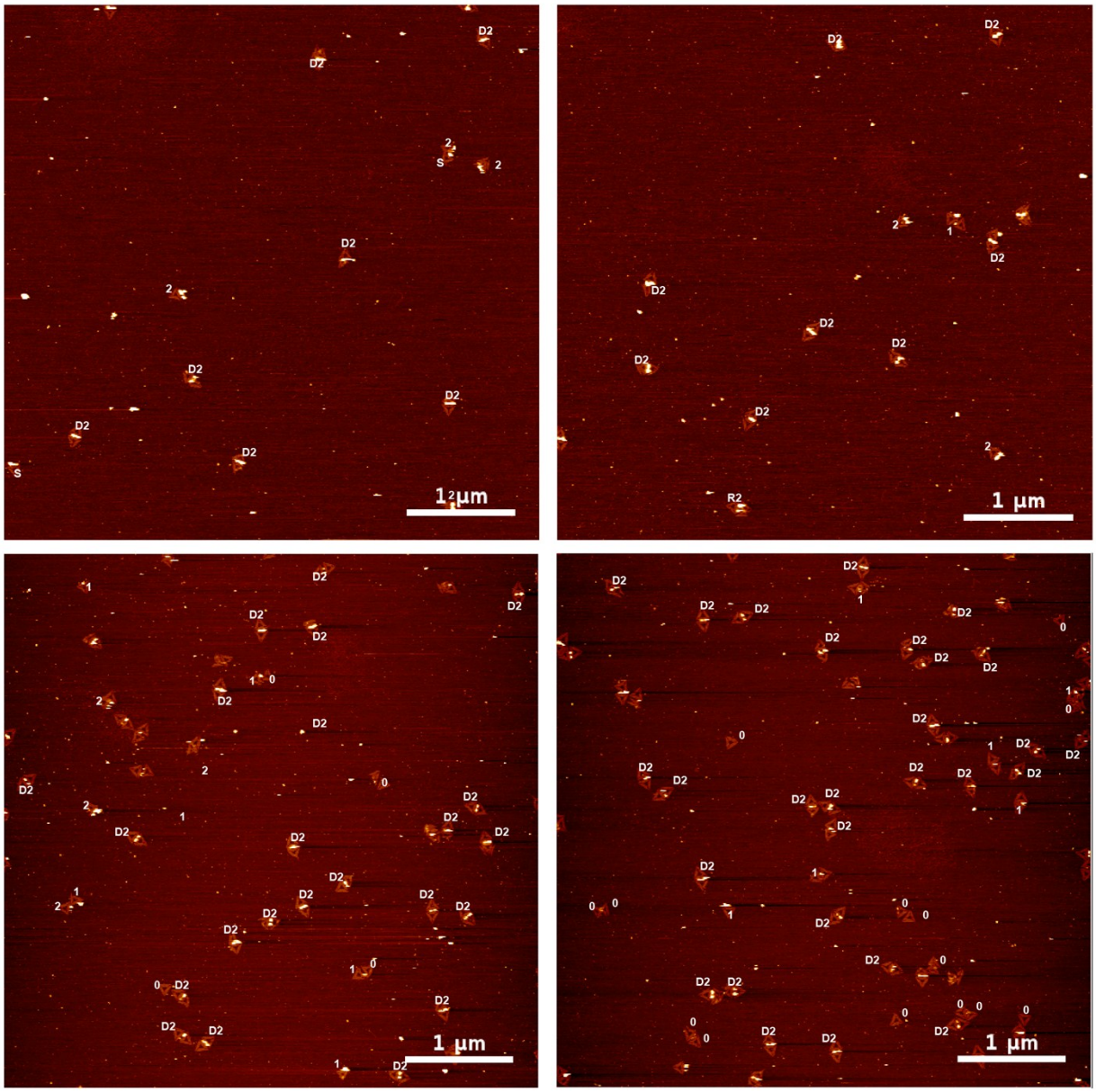

Figure S11: Representative AFM images of 20 X 50 nm AuNR ETE dimeric DNA triangle construct, including particle count analysis, the summary of which is shown in main text Figure 3.

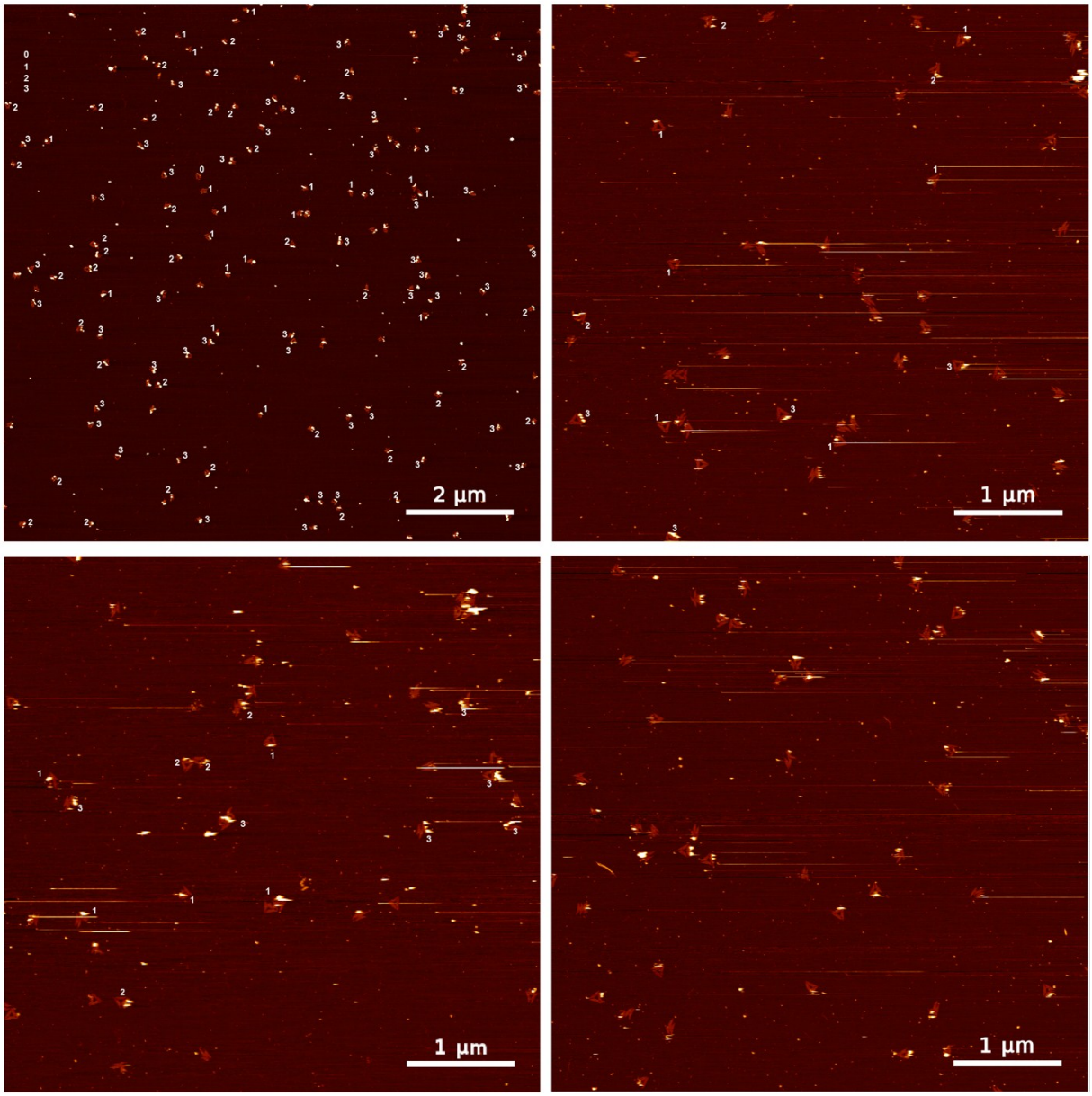

Figure S12: Representative AFM images of 20 X 50 nm AuNR RPR single DNA triangle construct, including particle count analysis, the summary of which is shown in main text Figure 4.

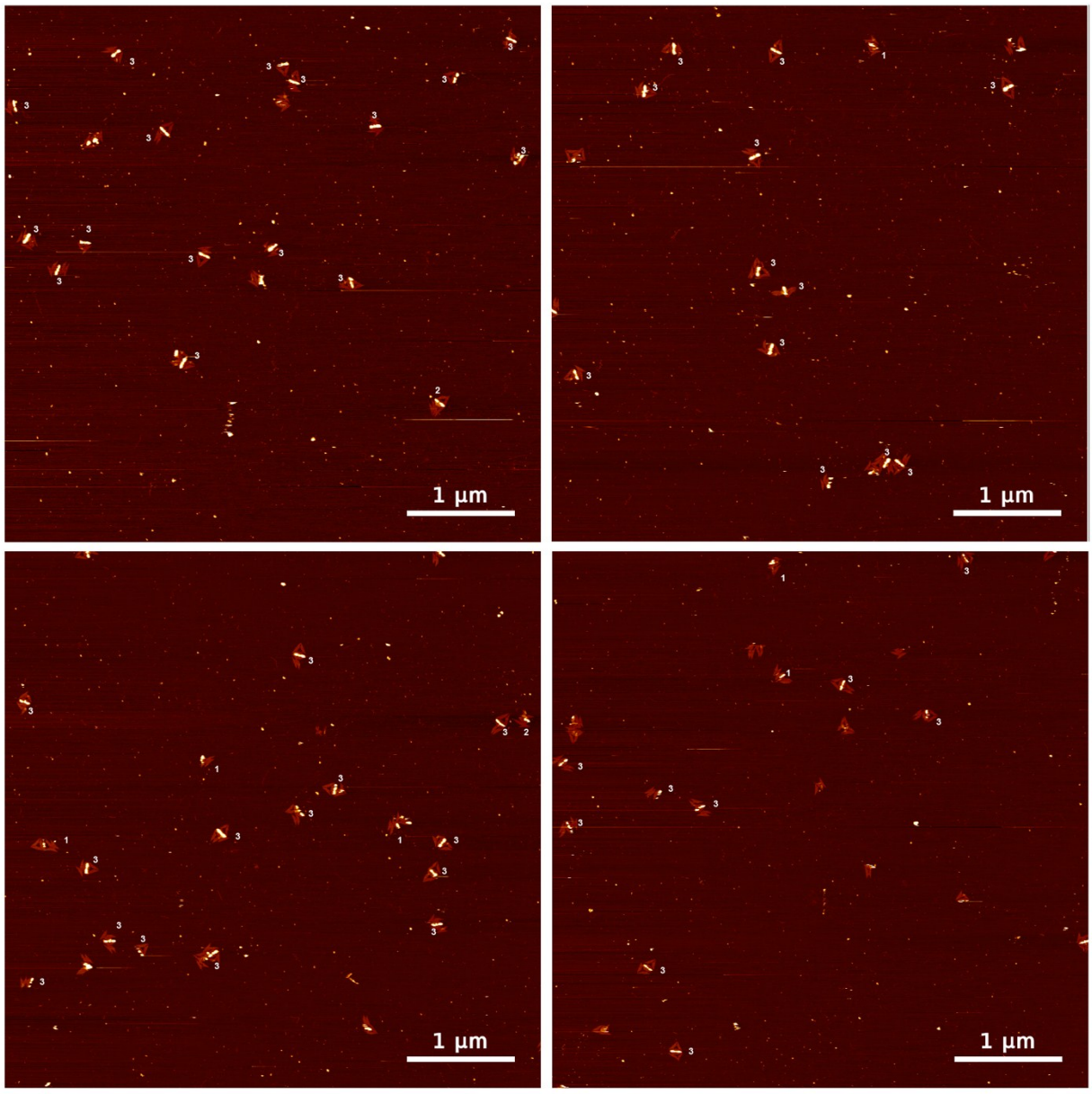

Figure S13: Representative AFM images of 20 X 50 nm AuNR RPR dimeric DNA triangle construct, including particle count analysis, the summary of which is shown in main text Figure 4.

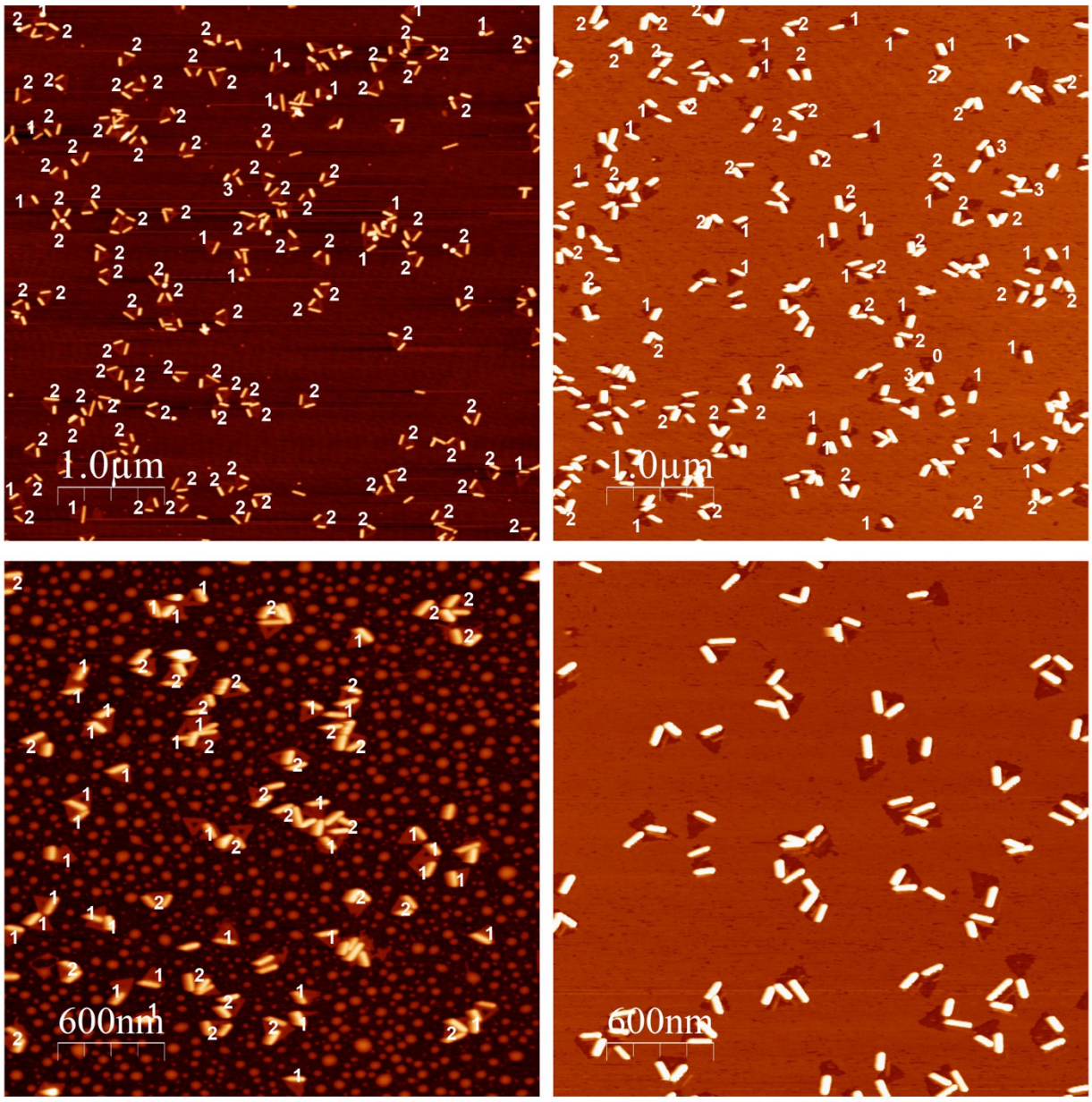

Figure S14: Representative AFM images of 90 nm AuNRs on the DNA triangle in inverted-V configuration, including particle count analysis, the summary of which is shown in main text Figure 5.

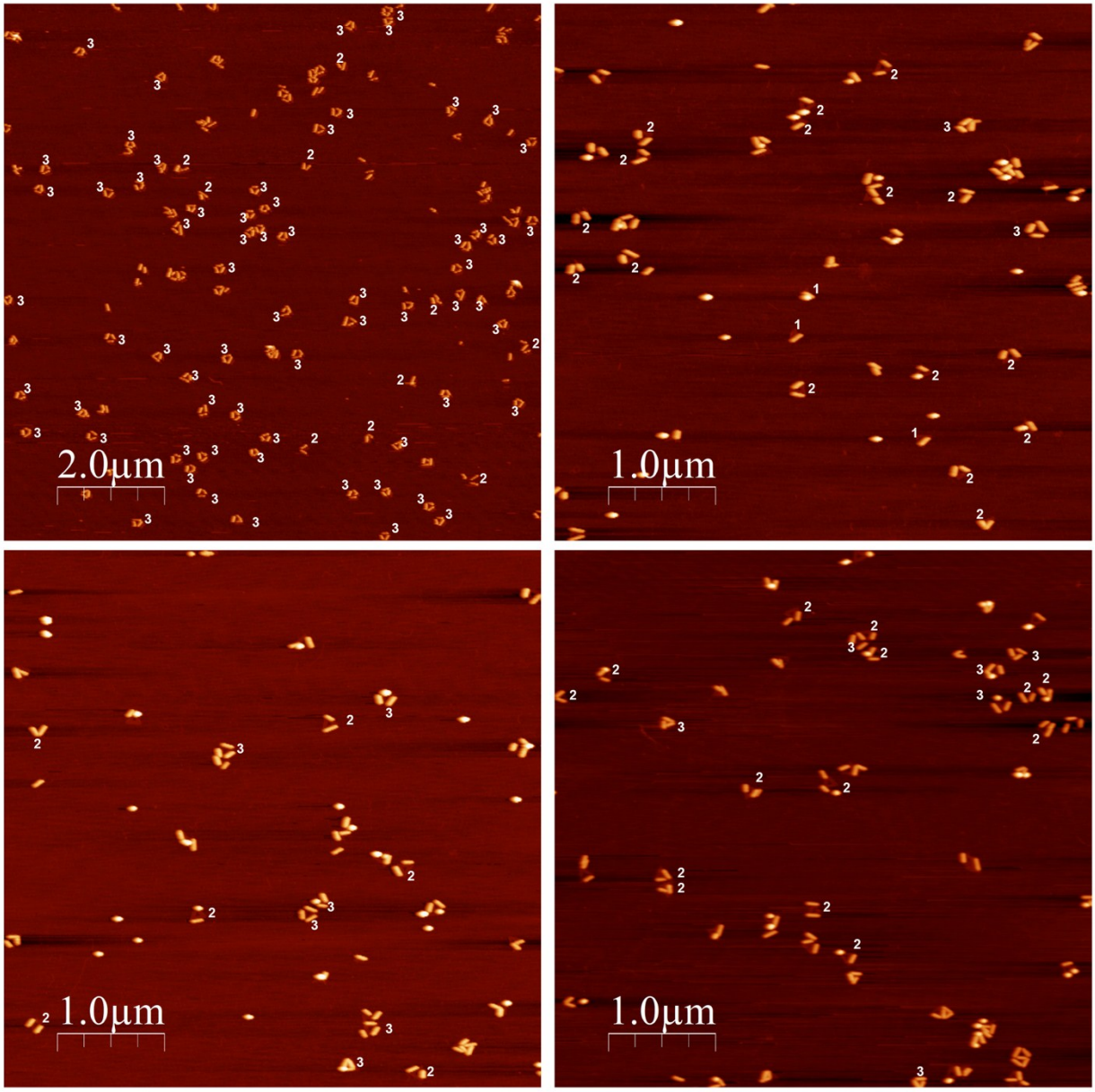

Figure S15: Representative AFM images of 90 nm AuNRs on the DNA triangle in three-rod-triangle configuration, including particle count analysis, the summary of which is included in main text Figure 5.

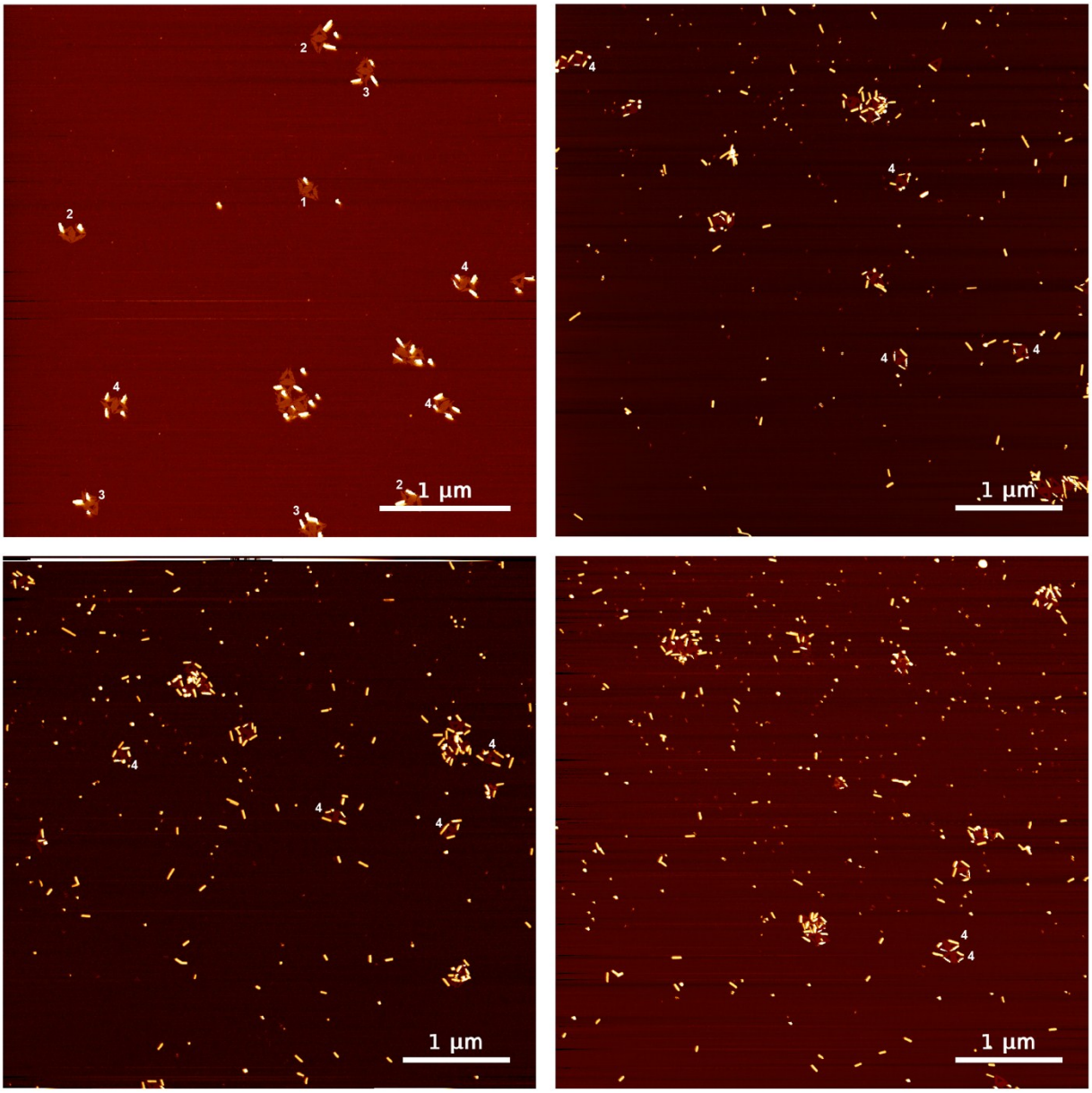

Figure S16: Representative AFM images of 90 nm AuNRs on the DNA rhombus, including particle count analysis, the summary of which is shown in main text Figure 6.

Supporting Information S6: Additional TEM images of each configuration

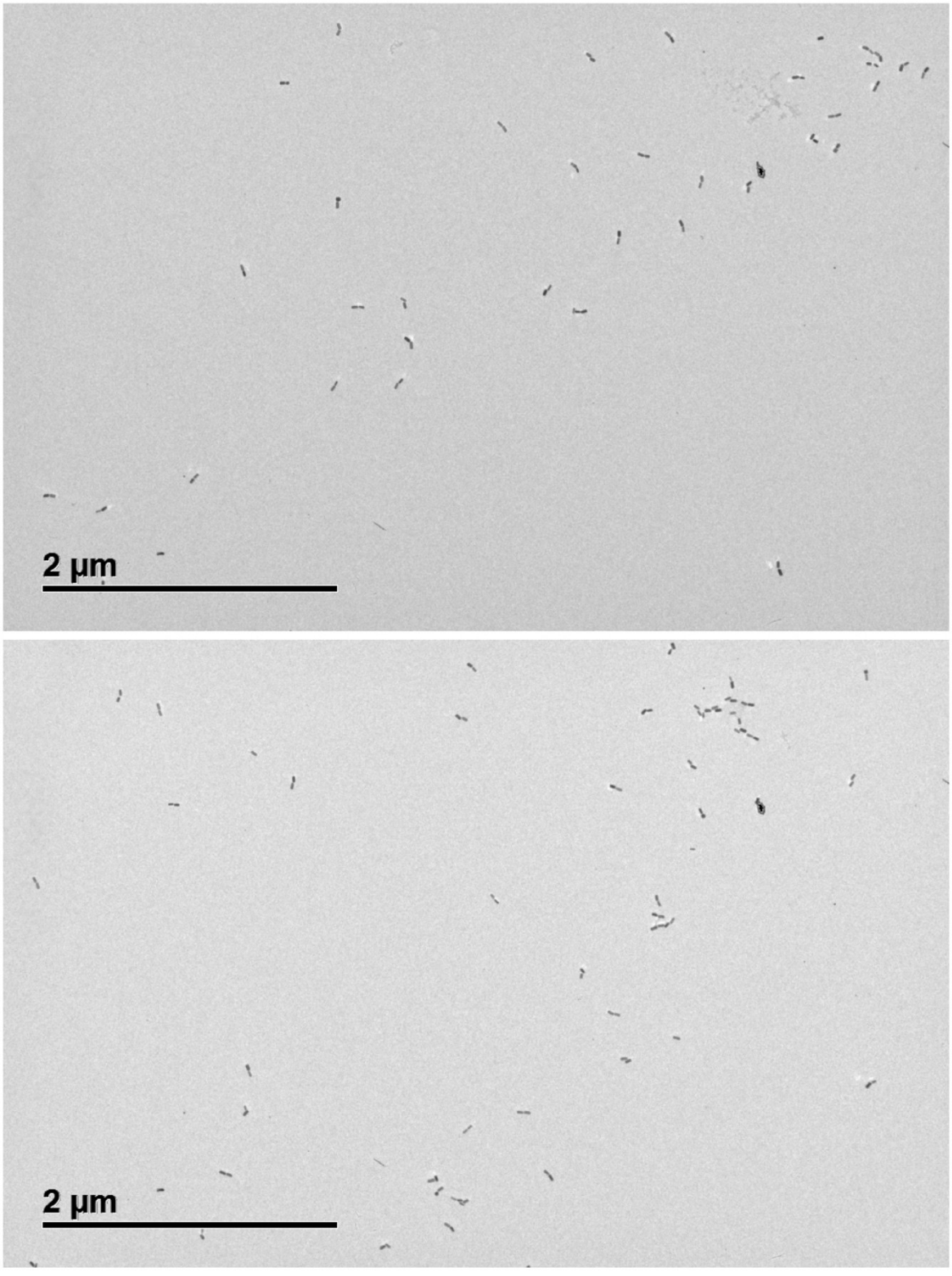

Figure S17: Representative TEM images of the ETE single triangle configuration.

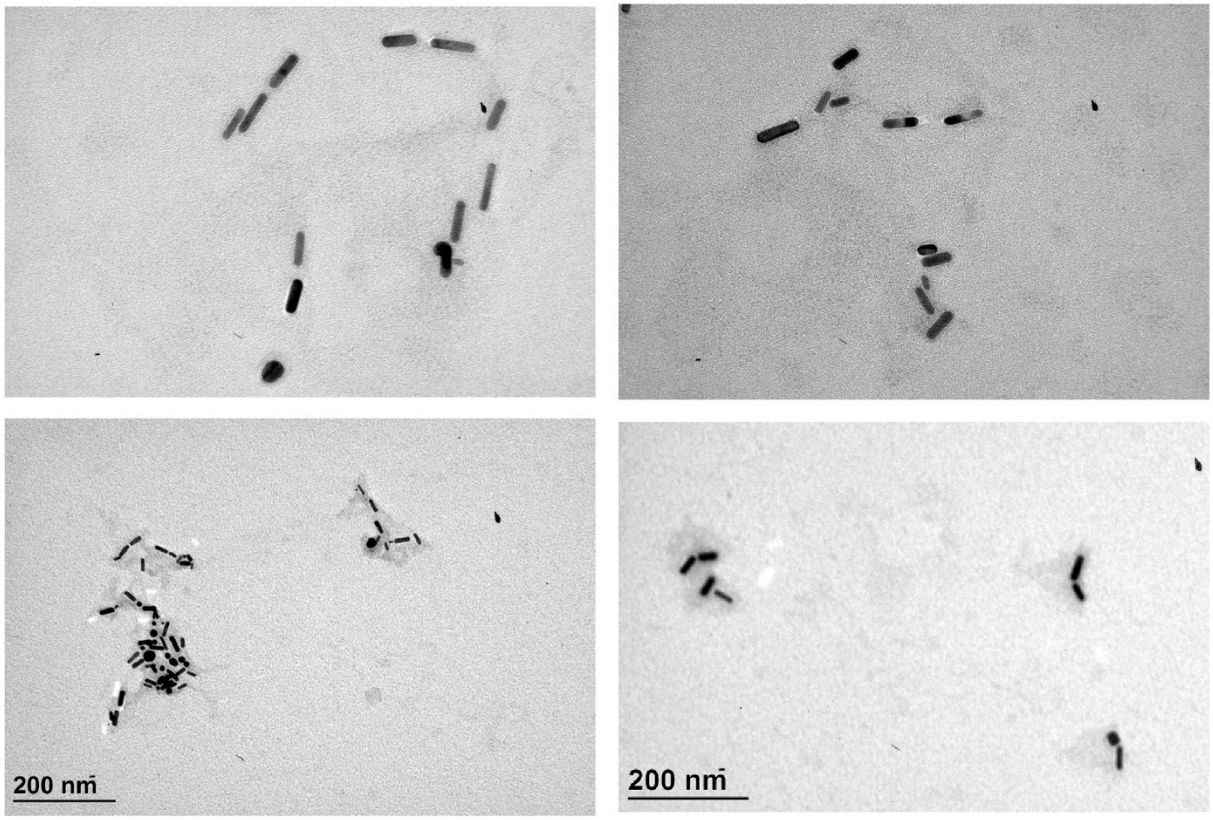

Figure S18: Representative TEM images of the ETE dimeric triangle configuration.

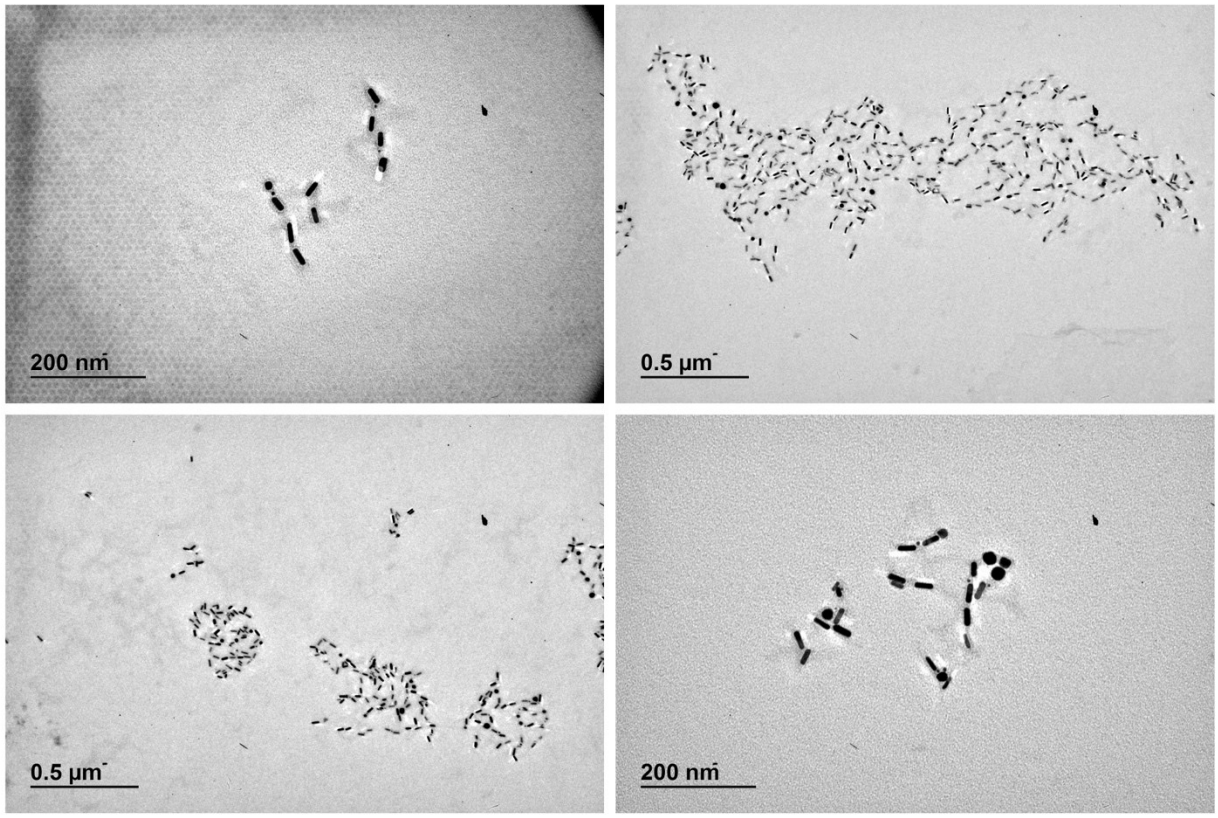

Figure S19: Representative TEM images of the RPR single triangle configuration.

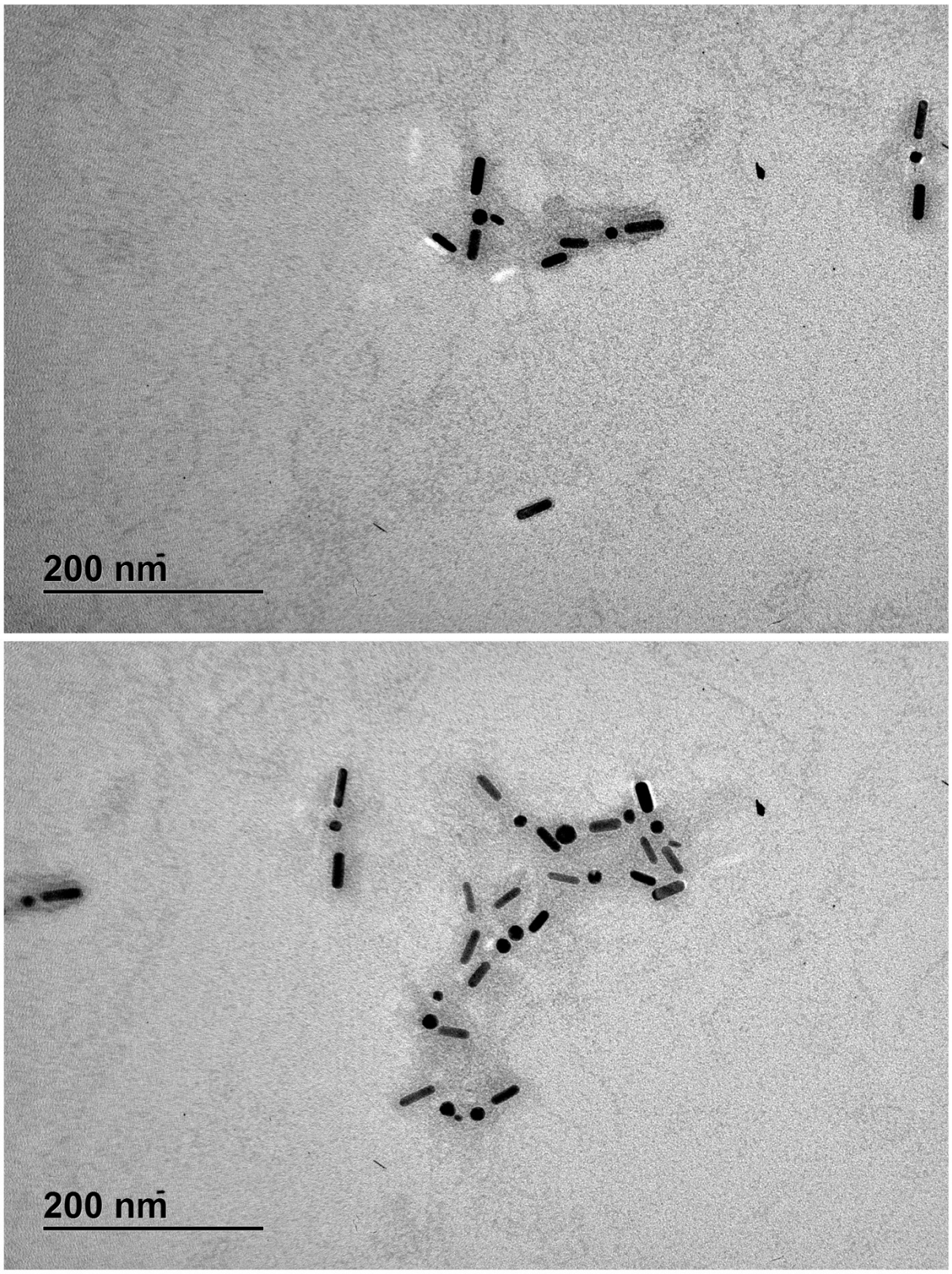

Figure S20: Representative TEM images of the RPR dimeric triangle configuration.

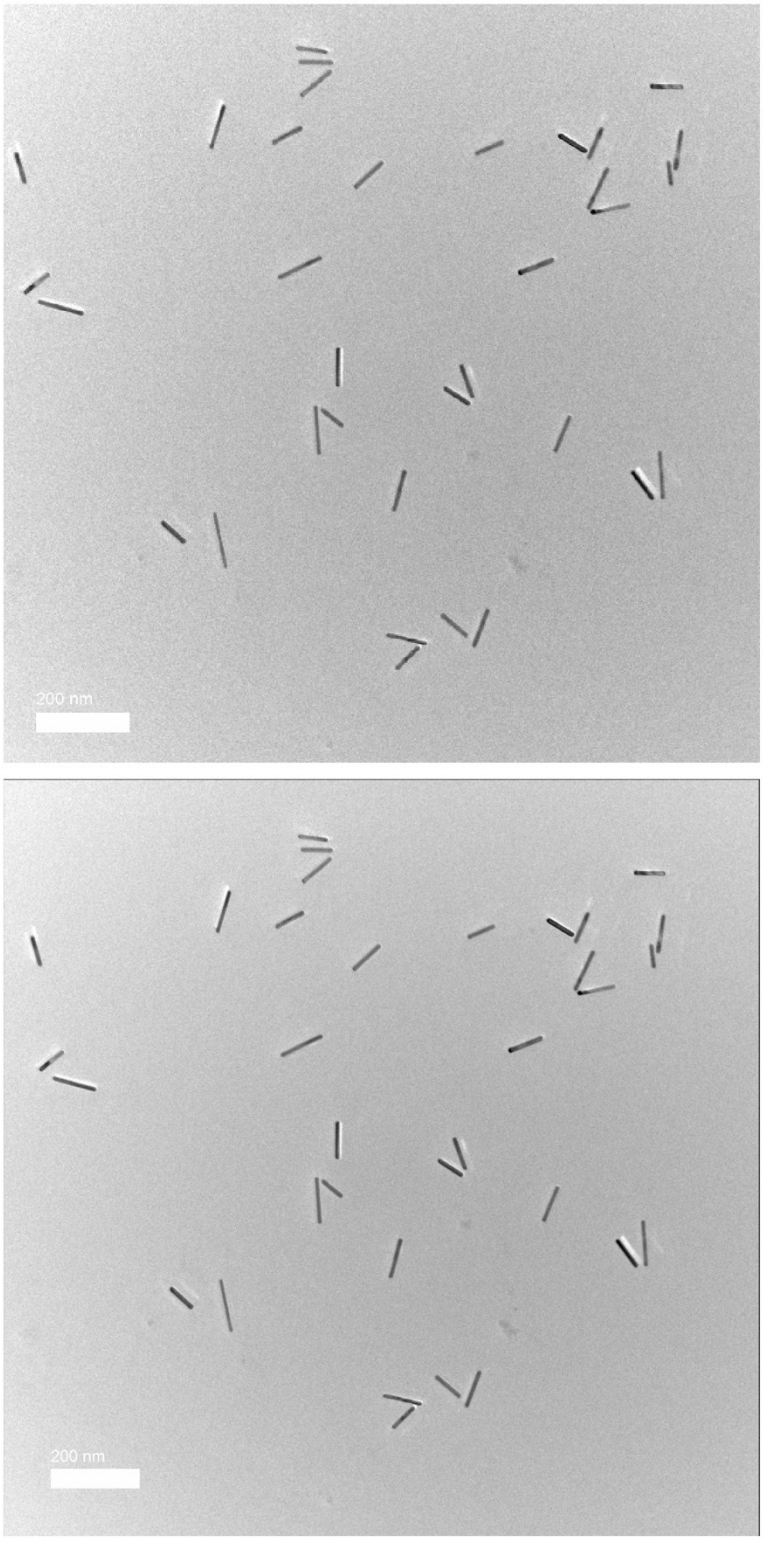

Figure S21: Representative TEM images of the inverted-V configuration.

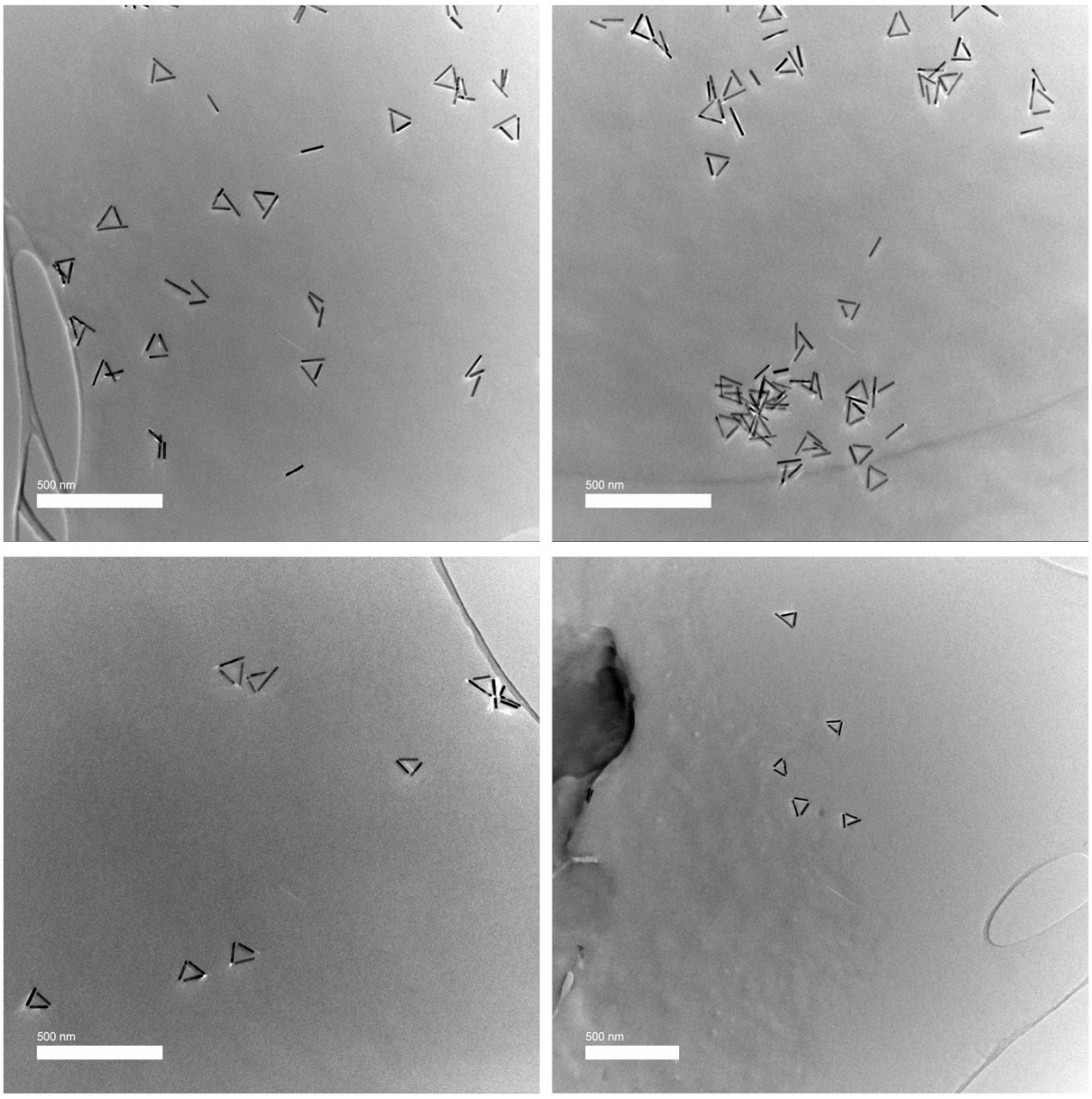

Figure S22: Representative TEM images of the three-rod-triangle configuration.

Supporting Information S7: COMSOL Simulations

AuNR configurations were arranged in various geometries in a box of water surrounded by Perfectly Matched Layers to absorb reflections. The dimer structure and the ETE and RPR configurations were composed of AuNRs that were 10 × 40 nm and AuNP with 10 nm diameter. The inverted-V, gold triangle, and diamond configurations were composed of AuRNs 10 × 90 nm. The nanostructures were specified as gold using the Rakić model for the refractive index.[10] The refractive index of water was taken to be n = 1.344.

A background electric field propagating in the x-direction and polarized in the z-direction was specified in the calculation to excite the plasmon mode: $E_{b,z} = E_0 exp(-ik_0 n_{water} x)$ where $E_{b,z}$ is the z-component of the background electric field, E_0 = 1 V/m, k_0 is the free space wavevector, and n_{med} is the refractive index of the medium. The nanostructures were oriented in such a way to ensure excitation of the LSPR. Absorption cross sections (σ_{abs}) were calculated by integrating the power dissipation, Q, over the volume of the nanorod: $\sigma_{abs} = \frac{\iiint Q}{P_{in}}$, where P_{in} is the input power, which is calculated as: $P_{in} = \frac{E_0^2}{2Z_0 n}$, where Z_0 is the characteristic impedance of vacuum. Scattering cross sections (σ_{scat}) were calculated by integrating the Poynting vector, S, over a surface surrounding the simulation domain (the boundary between the surrounding medium and the PML): $\sigma_{scat} = \frac{\iint S}{P_{in}}$. These results were then normalized such that the largest peak had a value of 1.

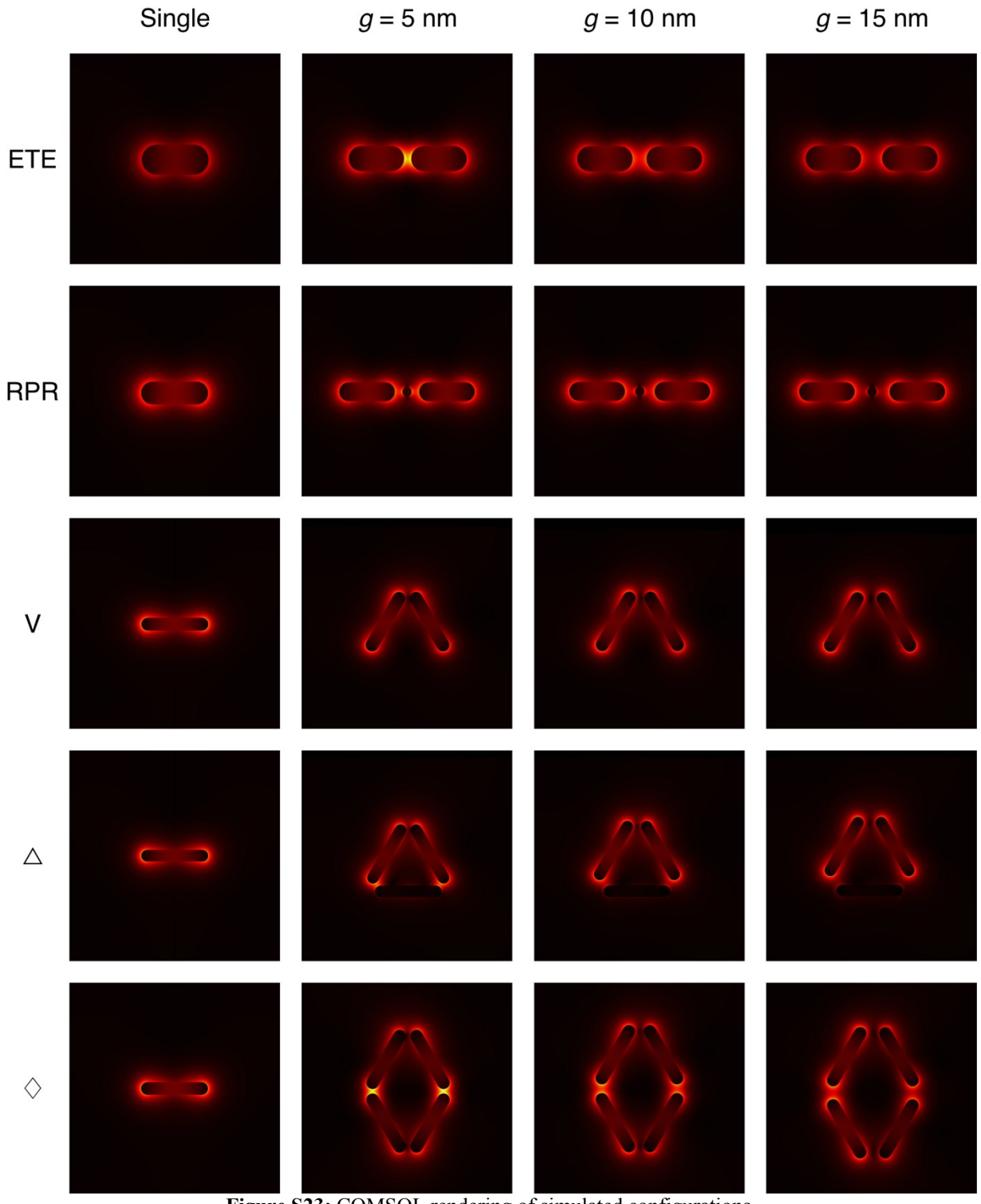

Figure S23: COMSOL rendering of simulated configurations.

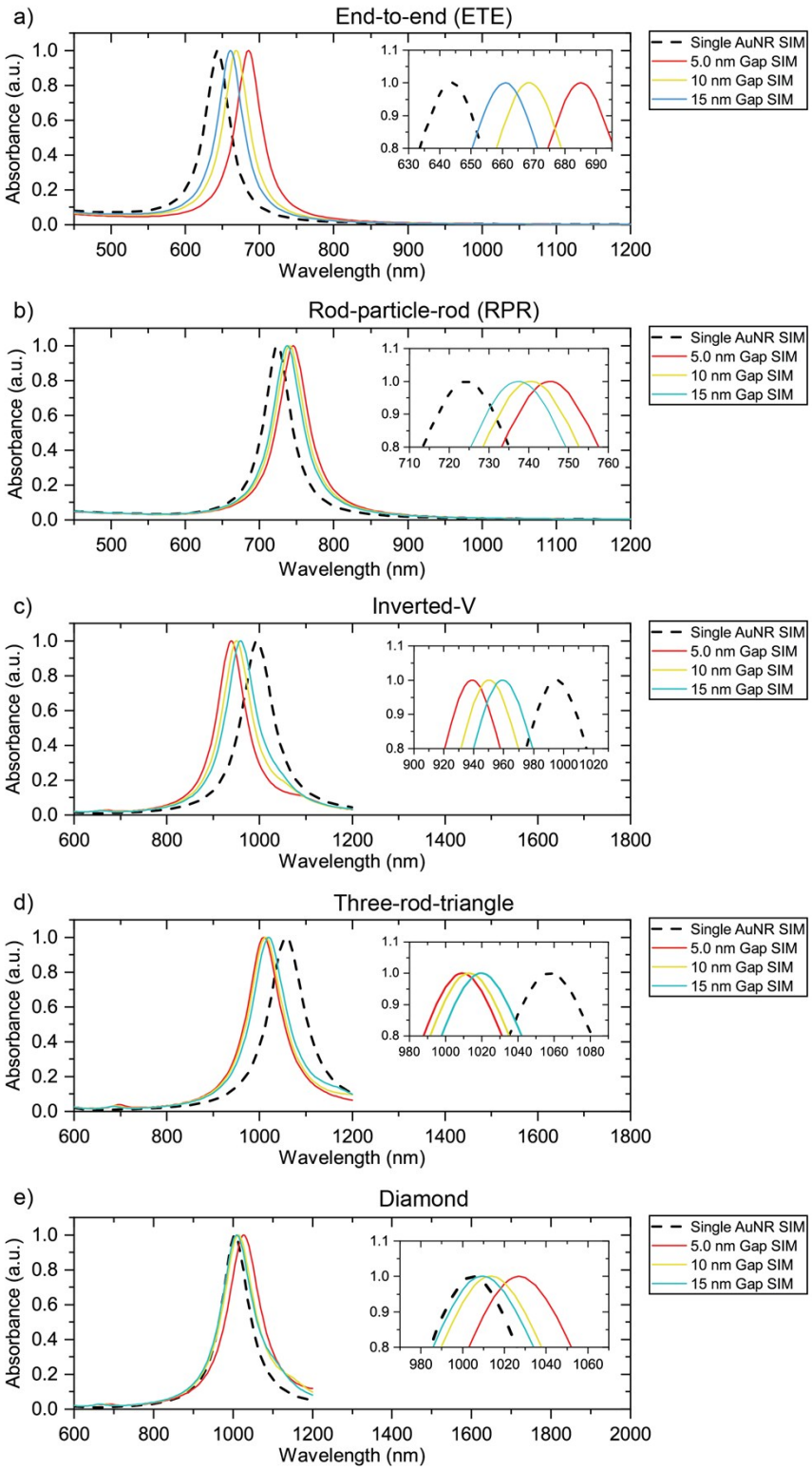

Figure S24: COMSOL simulations for inter-rod gaps of 5 nm, 10nm, and 15 nm in each configuration. (a) ETE, (b) RPR, (c) inverted-V, (d) three-rod-triangle, and (e) diamond configurations

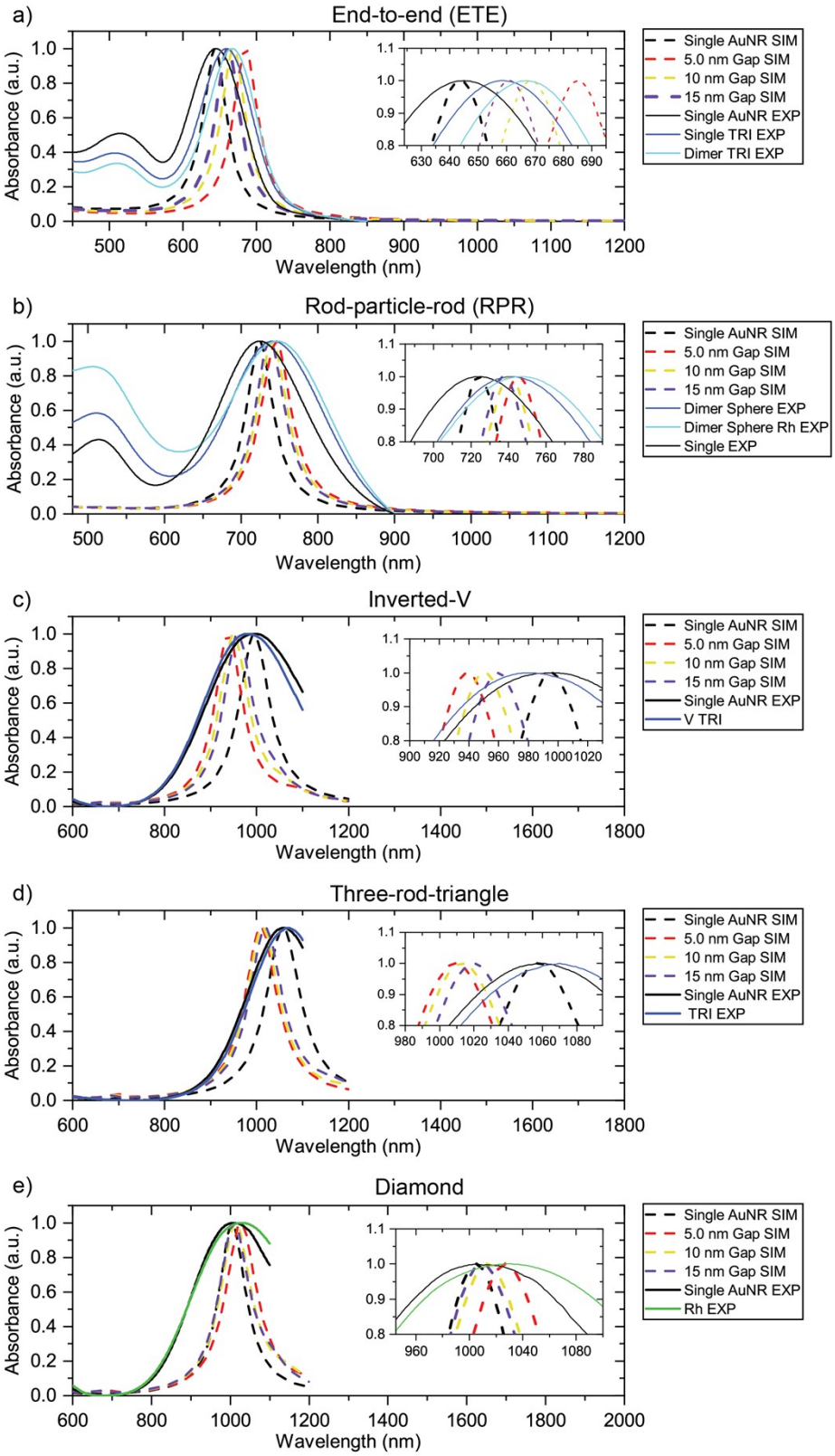

Figure S25: Experiment *versus* COMSOL simulations. (a) ETE, (b) RPR, (c) inverted-V, (d) three-rod-triangle, and (e) diamond configurations.

Supporting Information S8: DNA staple, bridge, and capture sequences.

T_m was calculated in accordance with the Salt Adjusted Melting Temperature Calculation:

$$T_m = 100.5 + \left(41 * \frac{yG + zC}{wA + xT + yG + zC}\right) - \left(\frac{820}{wA + xT + yG + zC}\right) + 16.6 * \log_{10}(2 * [Mg^{2+}])$$

*Where w,x,y,z are the number of the bases A,T,G,C in the sequence, respectively.
** $[Mg^{2+}]$ is in units of M.
Found at: *Kibbe WA. 'OligoCalc: an online oligonucleotide properties calculator'. (2007) Nucleic Acids Res. 35(webserver issue): May 25*

Table S1: Staple strands used for DNA triangle and rhombus nanostructures

Name	Sequence	T_M (℃)
A01	CGGGGTTTCCTCAAGAGAAGGATTTTGAATTA	62.6
A02	AGCGTCATGTCTCTGAATTTACCGACTACCTT	63.9
A03	TTCATAATCCCCTTATTAGCGTTTTTCTTACC	60.0
A04	ATGGTTTATGTCACAATCAATAGATATTAAAC	56.2
A05	TTTGATGATTAAGAGGCTGAGACTTGCTCAGTACCAGGCG	70.5
A06	CCGGAACCCAGAATGGAAAGCGCAACATGGCT	69.0
A07	AAAGACAACATTTTCGGTCATAGCCAAAATCA	60.0
A08	GACGGGAGAATTAACTCGGAATAAGTTTATTTCCAGCGCC	69.5
A09	GATAAGTGCCGTCGAGCTGAAACATGAAAGTATACAGGAG	69.5
A10	TGTACTGGAAATCCTCATTAAAGCAGAGCCAC	63.9
A11	CACCGGAAAGCGCGTTTTCATCGGAAGGGCGA	70.3
A12	CATTCAACAAACGCAAAGACACCAGAACACCCTGAACAAA	68.5
A13	TTTAACGGTTCGGAACCTATTATTAGGGTTGATATAAGTA	64.4
A14	CTCAGAGCATATTCACAAACAAATTAATAAGT	57.4
A15	GGAGGGAATTTAGCGTCAGACTGTCCGCCTCC	70.3
A16	GTCAGAGGGTAATTGATGGCAACATATAAAAGCGATTGAG	67.4
A17	TAGCCCGGAATAGGTGAATGCCCCCTGCCTATGGTCAGTG	74.6
A18	CCTTGAGTCAGACGATTGGCCTTGCGCCACCC	71.5
A19	TCAGAACCCAGAATCAAGTTTGCCGGTAAATA	62.6
A20	TTGACGGAAATACATACATAAAGGGCGCTAATATCAGAGA	66.4
A21	CAGAGCCAGGAGGTTGAGGCAGGTAACAGTGCCCG	73.9
A22	ATTAAAGGCCGTAATCAGTAGCGAGCCACCCT	66.4
A23	GATAACCCACAAGAATGTTAGCAAACGTAGAAAATTATTC	64.4
A24	GCCGCCAGCATTGACACCACCCTC	64.7
A25	AGAGCCGCACCATCGATAGCAGCATGAATTAT	65.1
A26	CACCGTCACCTTATTACGCAGTATTGAGTTAAGCCCAATA	68.5
A27	AGCCATTTAAACGTCACCAATGAACACCAGAACCA	65.7

A28	ATAAGAGCAAGAAACATGGCATGATTAAGACTCCGACTTG	67.4
A29	CCATTAGCAAGGCCGGGGGAATTA	59.6
A30	GAGCCAGCGAATACCCAAAAGAACATGAAATAGCAATAGC	68.5
A31	TATCTTACCGAAGCCCAAACGCAATAATAACGAAAATCACCAG	68.7
A32	CAGAAGGAAACCGAGGTTTTTAAGAAAAGTAAGCAGATAGCCG	69.6
A33	CCTTTTTTCATTTAACAATTTCATAGGATTAG	56.2
A34	TTTAACCTATCATAGGTCTGAGAGTTCCAGTA	61.3
A35	AGTATAAAATATGCGTTATACAAAGCCATCTT	57.4
A36	CAAGTACCTCATTCCAAGAACGGGAAATTCAT	62.6
A37	AGAGAATAACATAAAAACAGGGAAGCGCATTA	60.0
A38	AAAACAAAATTAATTAAATGGAAACAGTACATTAGTGAAT	59.2
A39	TTATCAAACCGGCTTAGGTTGGGTAAGCCTGT	65.1
A40	TTAGTATCGCCAACGCTCAACAGTCGGCTGTC	67.7
A41	TTTCCTTAGCACTCATCGAGAACAATAGCAGCCTTTACAG	68.5
A42	AGAGTCAAAAATCAATATATGTGATGAAACAAACATCAAG	62.3
A43	ACTAGAAATATATAACTATATGTACGCTGAGA	57.4
A44	TCAATAATAGGGCTTAATTGAGAATCATAATT	56.2
A45	AACGTCAAAAATGAAAAGCAAGCCGTTTTTATGAAACCAA	64.4
A46	GAGCAAAAGAAGATGAGTGAATAACCTTGCTTATAGCTTA	65.4
A47	GATTAAGAAATGCTGATGCAAATCAGAATAAA	57.4
A48	CACCGGAATCGCCATATTTAACAAAATTTACG	61.3
A49	AGCATGTATTTCATCGTAGGAATCAAACGATTTTTTGTTT	63.3
A50	ACATAGCGCTGTAAATCGTCGCTATTCATTTCAATTACCT	66.4
A51	GTTAAATACAATCGCAAGACAAAGCCTTGAAA	60.0
A52	CCCATCCTCGCCAACATGTAATTTAATAAGGC	63.9
A53	TCCCAATCCAAATAAGATTACCGCGCCCAATAAATAATAT	65.4
A54	TCCCTTAGAATAACGCGAGAAAACTTTTACCGACC	65.7
A55	GTGTGATAAGGCAGAGGCATTTTCAGTCCTGA	65.1
A56	ACAAGAAAGCAAGCAAATCAGATAACAGCCATATTATTTA	63.3
A57	GTTTGAAATTCAAATATATTTTAG	44.2
A58	AATAGATAGAGCCAGTAATAAGAGATTTAATG	57.4
A59	GCCAGTTACAAAATAATAGAAGGCTTATCCGGTTATCAAC	66.4
A60	TTCTGACCTAAAATATAAAGTACCGACTGCAGAAC	63.3
A61	GCGCCTGTTATTCTAAGAACGCGATTCCAGAGCCTAATTT	69.5
A62	TCAGCTAAAAAAGGTAAAGTAATT	47.6
A63	ACGCTAACGAGCGTCTGGCGTTTTAGCGAACCCAACATGT	72.6
A64	ACGACAATAAATCCCGACTTGCGGGAGATCCTGAATCTTACCA	71.5
A65	TGCTATTTTGCACCCAGCTACAATTTTGTTTTGAAGCCTTAAA	66.8
B01	TCATATGTGTAATCGTAAAACTAGTCATTTTC	57.4
B02	GTGAGAAAATGTGTAGGTAAAGATACAACTTT	58.7

B03	GGCATCAAATTTGGGGCGCGAGCTAGTTAAAG	66.4
B04	TTCGAGCTAAGACTTCAAATATCGGGAACGAG	63.9
B05	ACAGTCAAAGAGAATCGATGAACGACCCCGGTTGATAATC	69.5
B06	ATAGTAGTATGCAATGCCTGAGTAGGCCGGAG	66.4
B07	AACCAGACGTTTAGCTATATTTTCTTCTACTA	58.7
B08	GAATACCACATTCAACTTAAGAGGAAGCCCGATCAAAGCG	69.5
B09	AGAAAAGCCCCAAAAAGAGTCTGGAGCAAACAATCACCAT	68.5
B10	CAATATGACCCTCATATATTTTAAAGCATTAA	56.2
B11	CATCCAATAAATGGTCAATAACCTCGGAAGCA	62.6
B12	AACTCCAAGATTGCATCAAAAAGATAATGCAGATACATAA	63.3
B13	CGTTCTAGTCAGGTCATTGCCTGACAGGAAGATTGTATAA	68.5
B14	CAGGCAAGATAAAAATTTTTAGAATATTCAAC	56.2
B15	GATTAGAGATTAGATACATTTCGCAAATCATA	57.4
B16	CGCCAAAAGGAATTACAGTCAGAAGCAAAGCGCAGGTCAG	71.5
B17	GCAAATATTTAAATTGAGATCTACAAAGGCTACTGATAAA	62.3
B18	TTAATGCCTTATTTCAACGCAAGGGCAAAGAA	61.3
B19	TTAGCAAATAGATTTAGTTTGACCAGTACCTT	58.7
B20	TAATTGCTTTACCCTGACTATTATGAGGCATAGTAAGAGC	66.4
B21	ATAAAGCCTTTGCGGGAGAAGCCTGGAGAGGGTAG	70.4
B22	TAAGAGGTCAATTCTGCGAACGAGATTAAGCA	62.6
B23	AACACTATCATAACCCATCAAAAATCAGGTCTCCTTTTGA	65.4
B24	ATGACCCTGTAATACTTCAGAGCA	54.5
B25	TAAAGCTATATAACAGTTGATTCCCATTTTTG	57.4
B26	CGGATGGCACGAGAATGACCATAATCGTTTACCAGACGAC	71.5
B27	TAATTGCTTGGAAGTTTCATTCCAAATCGGTTGTA	62.2
B28	GATAAAAACCAAAATATTAAACAGTTCAGAAATTAGAGCT	61.3
B29	ACTAAAGTACGGTGTCGAATATAA	51.0
B30	TGCTGTAGATCCCCCTCAAATGCTGCGAGAGGCTTTTGCA	72.6
B31	AAAGAAGTTTTGCCAGCATAAATATTCATTGACTCAACATGTT	64.9
B32	AATACTGCGGAATCGTAGGGGGTAATAGTAAAATGTTTAGACT	67.7
B33	AGGGATAGCTCAGAGCCACCACCCCATGTCAA	69.0
B34	CAACAGTTTATGGGATTTTGCTAATCAAAAGG	60.0
B35	GCCGCTTTGCTGAGGCTTGCAGGGGAAAAGGT	70.3
B36	GCGCAGACTCCATGTTACTTAGCCCGTTTTAA	65.1
B37	ACAGGTAGAAAGATTCATCAGTTGAGATTTAG	60.0
B38	CCTCAGAACCGCCACCCAAGCCCAATAGGAACGTAAATGA	72.6
B39	ATTTTCTGTCAGCGGAGTGAGAATACCGATAT	62.6
B40	ATTCGGTCTGCGGGATCGTCACCCGAAATCCG	70.3
B41	CGACCTGCGGTCAATCATAAGGGAACGGAACAACATTATT	69.5
B42	AGACGTTACCATGTACCGTAACACCCCTCAGAACCGCCAC	73.6

B43	CACGCATAAGAAAGGAACAACTAAGTCTTTCC	62.6
B44	ATTGTGTCTCAGCAGCGAAAGACACCATCGCC	67.7
B45	TTAATAAAACGAACTAACCGAACTGACCAACTCCTGATAA	65.4
B46	AGGTTTAGTACCGCCATGAGTTTCGTCACCAGGATCTAAA	69.5
B47	GTTTTGTCAGGAATTGCGAATAATCCGACAAT	61.3
B48	GACAACAAGCATCGGAACGAGGGTGAGATTTG	66.4
B49	TATCATCGTTGAAAGAGGACAGATGGAAGAAAAATCTACG	66.4
B50	AGCGTAACTACAAACTACAACGCCTATCACCGTACTCAGG	70.5
B51	TAGTTGCGAATTTTTTCACGTTGATCATAGTT	58.7
B52	GTACAACGAGCAACGGCTACAGAGGATACCGA	67.7
B53	ACCAGTCAGGACGTTGGAACGGTGTACAGACCGAAACAAA	71.5
B54	ACAGACAGCCCAAATCTCCAAAAAAAAATTTCTTA	61.0
B55	AACAGCTTGCTTTGAGGACTAAAGCGATTATA	61.3
B56	CCAAGCGCAGGCGCATAGGCTGGCAGAACTGGCTCATTAT	74.6
B57	CGAGGTGAGGCTCCAAAAGGAGCC	63.0
B58	ACCCCCAGACTTTTTCATGAGGAACTTGCTTT	63.9
B59	ACCTTATGCGATTTTATGACCTTCATCAAGAGCATCTTTG	66.4
B60	CGGTTTATCAGGTTTCCATTAAACGGGAATACACT	64.5
B61	AAAACACTTAATCTTGACAAGAACTTAATCATTGTGAATT	61.3
B62	GGCAAAAGTAAAATACGTAATGCC	52.7
B63	TGGTTTAATTTCAACTCGGATATTCATTACCCACGAAAGA	65.4
B64	ACCAACCTAAAAAATCAACGTAACAAATAAATTGGGCTTGAGA	65.8
B65	CCTGACGAGAAACACCAGAACGAGTAGGCTGCTCATTCAGTGA	73.4
C01	TCGGGAGATATACAGTAACAGTACAAATAATT	58.7
C02	CCTGATTAAAGGAGCGGAATTATCTCGGCCTC	66.4
C03	GCAAATCACCTCAATCAATATCTGCAGGTCGA	63.9
C04	CGACCAGTACATTGGCAGATTCACCTGATTGC	66.4
C05	TGGCAATTTTTAACGTCAGATGAAAACAATAACGGATTCG	65.4
C06	AAGGAATTACAAAGAAACCACCAGTCAGATGA	61.3
C07	GGACATTCACCTCAAATATCAAACACAGTTGA	61.3
C08	TTGACGAGCACGTATACTGAAATGGATTATTTAATAAAAG	63.3
C09	CCTGATTGCTTTGAATTGCGTAGATTTTCAGGCATCAATA	66.4
C10	TAATCCTGATTATCATTTTGCGGAGAGGAAGG	62.6
C11	TTATCTAAAGCATCACCTTGCTGATGGCCAAC	63.9
C12	AGAGATAGTTTGACGCTCAATCGTACGTGCTTTCCTCGTT	69.5
C13	GATTATACACAGAAATAAAGAAATACCAAGTTACAAAATC	61.3
C14	TAGGAGCATAAAAGTTTGAGTAACATTGTTTG	58.7
C15	TGACCTGACAAATGAAAAATCTAAAATATCTT	56.2
C16	AGAATCAGAGCGGGAGATGGAAATACCTACATAACCCTTC	69.5
C17	GCGCAGAGGCGAATTAATTATTTGCACGTAAATTCTGAAT	66.4

C18	AATGGAAGCGAACGTTATTAATTTCTAACAAC	58.7
C19	TAATAGATCGCTGAGAGCCAGCAGAAGCGTAA	65.1
C20	GAATACGTAACAGGAAAAACGCTCCTAAACAGGAGGCCGA	70.5
C21	TCAATAGATATTAAATCCTTTGCCGGTTAGAACCT	62.2
C22	CAATATTTGCCTGCAACAGTGCCATAGAGCCG	66.4
C23	TTAAAGGGATTTTAGATACCGCCAGCCATTGCGGCACAGA	70.5
C24	ACAATTCGACAACTCGTAATACAT	51.0
C25	TTGAGGATGGTCAGTATTAACACCTTGAATGG	62.6
C26	CTATTAGTATATCCAGAACAATATCAGGAACGGTACGCCA	67.4
C27	CGCGAACTAAAACAGAGGTGAGGCTTAGAAGTATT	65.7
C28	GAATCCTGAGAAGTGTATCGGCCTTGCTGGTACTTTAATG	69.5
C29	ACCACCAGCAGAAGATGATAGCCC	59.6
C30	TAAAACATTAGAAGAACTCAAACTTTTTATAATCAGTGAG	61.3
C31	GCCACCGAGTAAAAGAACATCACTTGCCTGAGCGCCATTAAAA	71.5
C32	TCTTTGATTAGTAATAGTCTGTCCATCACGCAAATTAACCGTT	66.8
C33	CGCGTCTGATAGGAACGCCATCAACTTTTACA	65.1
C34	AGGAAGATGGGGACGACGACAGTAATCATATT	63.9
C35	CTCTAGAGCAAGCTTGCATGCCTGGTCAGTTG	67.7
C36	CCTTCACCGTGAGACGGGCAACAGCAGTCACA	70.3
C37	CGAGAAAGGAAGGGAAGCGTACTATGGTTGCT	66.4
C38	GCTCATTTTTTAACCAGCCTTCCTGTAGCCAGGCATCTGC	71.5
C39	CAGTTTGACGCACTCCAGCCAGCTAAACGACG	69.0
C40	GCCAGTGCGATCCCCGGGTACCGAGTTTTTCT	70.3
C41	TTTCACCAGCCTGGCCCTGAGAGAAAGCCGGCGAACGTGG	76.7
C42	GTAACCGTCTTTCATCAACATTAAAATTTTTGTTAAATCA	61.3
C43	ACGTTGTATTCCGGCACCGCTTCTGGCGCATC	70.3
C44	CCAGGGTGGCTCGAATTCGTAATCCAGTCACG	69.0
C45	TAGAGCTTGACGGGGAGTTGCAGCAAGCGGTCATTGGGCG	75.6
C46	GTTAAAATTCGCATTAATGTGAGCGAGTAACACACGTTGG	67.4
C47	TGTAGATGGGTGCCGGAAACCAGGAACGCCAG	70.3
C48	GGTTTTCCATGGTCATAGCTGTTTGAGAGGCG	66.4
C49	GTTTGCGTCACGCTGGTTTGCCCCAAGGGAGCCCCCGATT	76.7
C50	GGATAGGTACCCGTCGGATTCTCCTAAACGTTAATATTTT	67.4
C51	AGTTGGGTCAAAGCGCCATTCGCCCCGTAATG	69.0
C52	CGCGCGGGCCTGTGTGAAATTGTTGGCGATTA	69.0
C53	CTAAATCGGAACCCTAAGCAGGCGAAAATCCTTCGGCCAA	71.5
C54	CGGCGGATTGAATTCAGGCTGCGCAACGGGGGATG	73.9
C55	TGCTGCAAATCCGCTCACAATTCCCAGCTGCA	67.7
C56	TTAATGAAGTTTGATGGTGGTTCCGAGGTGCCGTAAAGCA	69.5
C57	TGGCGAAATGTTGGGAAGGGCGAT	59.6

C58	TGTCGTGCACACAACATACGAGCCACGCCAGC	70.3
C59	CAAGTTTTTTGGGGTCGAAATCGGCAAAATCCGGGAAACC	70.5
C60	TCTTCGCTATTGGAAGCATAAAGTGTATGCCCGCT	66.9
C61	TTCCAGTCCTTATAAATCAAAAGAGAACCATCACCCAAAT	65.4
C62	GCGCTCACAAGCCTGGGGTGCCTA	64.7
C63	CGATGGCCCACTACGTATAGCCCGAGATAGGGATTGCGTT	73.6
C64	AACTCACATTATTGAGTGTTGTTCCAGAAACCGTCTATCAGGG	69.6
C65	ACGTGGACTCCAACGTCAAAGGGCGAATTTGGAACAAGAGTCC	73.4
Link-A1C	TTAATTAATTTTTTACCATATCAAA	43.7
Link-A2C	TTAATTTCATCTTAGACTTTACAA	45.9
Link-A3C	CTGTCCAGACGTATACCGAACGA	57.3
Link-A4C	TCAAGATTAGTGTAGCAATACT	47.3
Link-B1A	TGTAGCATTCCTTTTATAAACAGTT	50.2
Link-B2A	TTTAATTGTATTTCCACCAGAGCC	52.7
Link-B3A	ACTACGAAGGCTTAGCACCATTA	53.7
Link-B4A	ATAAGGCTTGCAACAAAGTTAC	49.2
Link-C1B	GTGGGAACAAATTTCTATTTTTGAG	51.9
Link-C2B	CGGTGCGGGCCTTCCAAAAACATT	59.6
Link-C3B	ATGAGTGAGCTTTTAAATATGCA	48.4
Link-C4B	ACTATTAAAGAGGATAGCGTCC	51.0
Loop	GCGCTTAATGCGCCGCTACAGGGC	64.7

Table S2: Bridge staple strands required to assemble the DNA rhombus.

Name	**Sequence**	**T_M (℃)**
B45-A	ACGAACTAACCGAACTGACCAACTCCTGATAA	63.9
B53-A	GGACGTTGGAACGGTGTACAGACCGAAACAAA	66.4
B59-A	CGATTTTATGACCTTCATCAAGAGCATCTTTG	61.3
B63-A	TTTCAACTCGGATATTCATTACCCACGAAAGA	61.3
B12-D	AACTCCAAGATTGCATCAAAAAGATAATGCAGATACATAATTAATAAA	64.7
B20-D	TAATTGCTTTACCCTGACTATTATGAGGCATAGTAAGAGCACCAGTCA	70.7
B26-D	CGGATGGCACGAGAATGACCATAATCGTTTACCAGACGACACCTTATG	74.1
B30-D	TGCTGTAGATCCCCCTCAAATGCTGCGAGAGGCTTTTGCATGGTTTAA	74.1

Table S3: Thiol-labeled DNA strands used for the functionalization of AuNR and AuNP.

Name	**Sequence**
A-seq	TTTTTTTTTTTTTTTTAGCGA/3ThioMC3-D/
Q-seq	GATTCGATAGCTTATGCTGC/3ThioMC3-D/

Table S4: List of capture strands used for AuNR/AuNP attachment.

Name	Modification	Sequence	T_M (℃)
Complementary to A-seq-thiol DNA			
Side A			
AA04	Tri-Aseq-A04	AAAAAAAAAAAAAAAAATGGTTTATGTCACAATCAATAGATATTAAAC	61.1
AA08	Tri-Aseq-A08	AAAAAAAAAAAAAAAAGACGGGAGAATTAACTCGGAATAAGTTTATTTCCAGCGCC	70.0
AA12	Tri-Aseq-A12	AAAAAAAAAAAAAAAACATTCAACAAACGCAAAGACACCAGAACACCCTGAACAAA	69.3
AA16	Tri-Aseq-A16	AAAAAAAAAAAAAAAAGTCAGAGGGTAATTGATGGCAACATATAAAAGCGATTGAG	68.6
AA20	Tri-Aseq-A20	AAAAAAAAAAAAAAAATTGACGGAAATACATACATAAAGGGCGCTAATATCAGAGA	67.8
AA23	Tri-Aseq-A23	AAAAAAAAAAAAAAAAGATAACCCACAAGAATGTTAGCAAACGTAGAAAATTATTC	66.3
AA26	Tri-Aseq-A26	AAAAAAAAAAAAAAAACACCGTCACCTTATTACGCAGTATTGAGTTAAGCCCAATA	69.3
AA28	Tri-Aseq-A28	AAAAAAAAAAAAAAAAATAAGAGCAAGAAACATGGCATGATTAAGACTCCGACTTG	68.6
AA30	Tri-Aseq-A30	AAAAAAAAAAAAAAAAGAGCCAGCGAATACCCAAAAGAACATGAAATAGCAATAGC	69.3
AA31	Tri-Aseq-A31	AAAAAAAAAAAAAAAATATCTTACCGAAGCCCAAACGCAATAATAACGAAAATCACCAG	69.4
AA37	Tri-Aseq-A37	AAAAAAAAAAAAAAAAAGAGAATAACATAAAAACAGGGAAGCGCATTA	63.7
AA41	Tri-Aseq-A41	AAAAAAAAAAAAAAAATTTCCTTAGCACTCATCGAGAACAATAGCAGCCTTTACAG	69.3
AA45	Tri-Aseq-A45	AAAAAAAAAAAAAAAAAACGTCAAAAATGAAAAGCAAGCCGTTTTTATGAAACCAA	66.3
AA49	Tri-Aseq-A49	AAAAAAAAAAAAAAAAAGCATGTATTTCATCGTAGGAATCAAACGATTTTTTGTTT	65.6
AA53	Tri-Aseq-A53	AAAAAAAAAAAAAAAATCCCAATCCAAATAAGATTACCGCGCCCAATAAATAATAT	67.1
AA56	Tri-Aseq-A56	AAAAAAAAAAAAAAAAACAAGAAAGCAAGCAAATCAGATAACAGCCATATTATTTA	65.6
AA59	Tri-Aseq-A59	AAAAAAAAAAAAAAAAGCCAGTTACAAAATAATAGAAGGCTTATCCGGTTATCAAC	67.8
AA61	Tri-Aseq-A61	AAAAAAAAAAAAAAAAGCGCCTGTTATTCTAAGAACGCGATTCCAGAGCCTAATTT	70.0
AA62	Tri-Aseq-A62	AAAAAAAAAAAAAAAATCAGCTAAAAAAGGTAAAGTAATT	56.8
AA63	Tri-Aseq-A63	AAAAAAAAAAAAAAAAACGCTAACGAGCGTCTGGCGTTTTAGCGAACCCAACATGT	72.3
Side B			
AB04	Tri-Aseq-B04	AAAAAAAAAAAAAAAATTCGAGCTAAGACTTCAAATATCGGGAACGAG	66.3
AB12	Tri-Aseq-B12	AAAAAAAAAAAAAAAAAACTCCAAGATTGCATCAAAAAGATAATGCAGATACATAA	65.6
AB20	Tri-Aseq-B20	AAAAAAAAAAAAAAAATAATTGCTTTACCCTGACTATTATGAGGCATAGTAAGAGC	67.8
AB26	Tri-Aseq-B26	AAAAAAAAAAAAAAAACGGATGGCACGAGAATGACCATAATCGTTTACCAGACGAC	71.5
AB30	Tri-Aseq-B30	AAAAAAAAAAAAAAAATGCTGTAGATCCCCCTCAAATGCTGCGAGAGGCTTTTGCA	72.3
AB41	Tri-Aseq-B41	AAAAAAAAAAAAAAAACGACCTGCGGTCAATCATAAGGGAACGGAACAACATTATT	70.0
AB49	Tri-Aseq-B49	AAAAAAAAAAAAAAAATATCATCGTTGAAAGAGGACAGATGGAAGAAAAATCTACG	67.8
AB56	Tri-Aseq-B56	AAAAAAAAAAAAAAAACCAAGCGCAGGCGCATAGGCTGGCAGAACTGGCTCATTAT	73.8
AB61	Tri-Aseq-B61	AAAAAAAAAAAAAAAAAAACACTTAATCTTGACAAGAACTTAATCATTGTGAATT	64.1
AB62	Tri-Aseq-B62	AAAAAAAAAAAAAAAAGGCAAAAGTAAAATACGTAATGCC	60.0
Side C			

AC04	Tri-Aseq-C04	AAAAAAAAAAAAAAACGACCAGTACATTGGCAGATTCACCTGATTGC	68.0
AC12	Tri-Aseq-C12	AAAAAAAAAAAAAAAAAGAGATAGTTTGACGCTCAATCGTACGTGCTTTCCTCGTT	70.0
AC20	Tri-Aseq-C20	AAAAAAAAAAAAAAAAGAATACGTAACAGGAAAAACGCTCCTAAACAGGAGGCCGA	70.8
AC26	Tri-Aseq-C26	AAAAAAAAAAAAAAAACTATTAGTATATCCAGAACAATATCAGGAACGGTACGCCA	68.6
AC30	Tri-Aseq-C30	AAAAAAAAAAAAAAAATAAAACATTAGAAGAACTCAAACTTTTTATAATCAGTGAG	64.1
AC41	Tri-Aseq-C41	AAAAAAAAAAAAAAAATTTCACCAGCCTGGCCCTGAGAGAAAGCCGGCGAACGTGG	75.3
AC49	Tri-Aseq-C49	AAAAAAAAAAAAAAAATTGTTTGCGTCACGCTGGTTTGCCCCAAGGGAGCCCCCGATT	75.1
AC56	Tri-Aseq-C56	AAAAAAAAAAAAAAAATTTTAATGAAGTTTGATGGTGGTTCCGAGGTGCCGTAAAGCA	70.1
AC61	Tri-Aseq-C61	AAAAAAAAAAAAAAAATTCCAGTCCTTATAAATCAAAAGAGAACCATCACCCAAAT	67.1
AC62	Tri-Aseq-C62	AAAAAAAAAAAAAAAAGCGCTCACAAGCCTGGGGTGCCTA	67.3
Complementary to Q-seq-thiol DNA			
QA04	Tri-Qseq-A04	ATAAGCTATCGAATCATGGTTTATGTCACAATCAATAGATATTAAAC	65.4
QA08	Tri-Qseq-A08	ATAAGCTATCGAATCGACGGGAGAATTAACTCGGAATAAGTTTATTTCCAGCGCC	73.8
QA36	Tri-Qseq-A36	ATAAGCTATCGAATCCAAGTACCTCATTCCAAGAACGGGAAATTCAT	69.8
QA37	Tri-Qseq-A37	ATAAGCTATCGAATCAGAGAATAACATAAAAACAGGGAAGCGCATTA	68.0

Table S5: Ratio of AuNR/AuNP to DNA origami template.

Arrangement	AuNR	AuNP
End-to-end	10-20X	
Rod-particle-rod	10-20X	20X
Inverted-V	20X	
Three-rod-triangle	30X	
Diamond	20X	

Table S6: Capture strand positions corresponding to each AuNR configuration.

Configuration	AuNR Length	Thiol-sequence	Capture strand positions
ETE	40 nm	A seq	AA08, AA16, AA23, AA28, AA37, AA45, AA53, AA59
RPR	40 nm	A seq, Q seq	AQ04, AQ08, AA16, AA23, AA28, AA31, AQ36, AQ37, AA45, AA53, AA59, AA63
Inverted-V	90 nm	A seq	AA04, AA12, AA20, AA26, AA30, AA41, AA49, AA56, AA61, AA62, AC04, AC12, AC20, AC26, AC30, AC41, AC49, AC56, AC61, AC62
Three-rod-triangle	90 nm	A seq	AA04, AA12, AA20, AA26, AA30, AA41, AA49, AA56, AA61, AA62, AC04, AC12, AC20, AC26, AC30, AC41, AC49, AC56, AC61, AC62, AB04, AB12, AB20, AB26, AB30, AB41, AB49, AB56, AB61, AB62
Diamond	90 nm	A seq	AA04, AA12, AA20, AA26, AA30, AA41, AA49, AA56, AA61, AA62, AC04, AC12, AC20, AC26, AC30, AC41, AC49, AC56, AC61, AC62

References

1. P. W. K. Rothemund, *Nature*, 2006, **440**, 297-302.
2. S. M. Douglas, A. H. Marblestone, S. Teerapittayanon, A. Vazquez, G. M. Church and W. M. Shih, *Nucleic Acids Res.*, 2009, **37**, 5001-5006.
3. E. Oh, D. Lee, Y. P. Kim, S. Y. Cha, D. B. Oh, H. A. Kang, J. Kim and H. S. Kim, *Angew. Chem., Int. Ed.*, 2006, **45**, 7959-7963.
4. E. Oh, K. Susumu, R. Goswami and H. J. L. Mattoussi, *Langmuir*, 2010, **26**, 7604-7613.
5. K. Susumu, E. Oh, J. B. Delehanty, J. B. Blanco-Canosa, B. J. Johnson, V. Jain, W. J. Hervey IV, W. R. Algar, K. Boeneman and P. E. Dawson, *J. Am. Chem. Soc*, 2011, **133**, 9480-9496.
6. E. Oh, J. B. Delehanty, K. E. Sapsford, K. Susumu, R. Goswami, J. B. Blanco-Canosa, P. E. Dawson, J. Granek, M. Shoff and Q. J. A. n. Zhang, *ACS Nano*, 2011, **5**, 6434-6448.
7. J. Fontana, R. Nita, N. Charipar, J. Naciri, K. Park, A. Dunkelberger, J. Owrutsky, A. Piqué, R. Vaia and B. Ratna, *Adv. Opt. Mater.*, 2017, **5**, 1700335.
8. H. Jia, C. Fang, X.-M. Zhu, Q. Ruan, Y.-X. J. Wang and J. J. L. Wang, *Langmuir*, 2015, **31**, 7418-7426.
9. X. Zhang, M. R. Servos and J. Liu, *J. Am. Chem. Soc*, 2012, **134**, 7266-7269.
10. A. D. Rakić, A. B. Djurišić, J. M. Elazar and M. L. Majewski, *Appl. Opt.*, 1998, **37**, 5271-5283.